Late Cenozoic crustal extension and magmatism, southern Death Valley region, California

J.P. Calzia
U.S. Geological Survey, 345 Middlefield Road, Menlo Park, California 94025 USA
O.T. Rämö
Department of Geology, University of Helsinki, P.O. Box 11, FIN-00014, Finland

ABSTRACT

The late Cenozoic geologic history of the southern Death Valley region is characterized by coeval crustal extension and magmatism. Crustal extension is accommodated by numerous listric and planar normal faults as well as right- and left-lateral strike slip faults. The normal faults dip 30°–50°W near the surface and flatten and merge at depth into a detachment zone at or near the contact between Proterozoic cratonic rocks and Proterozoic and Paleozoic miogeoclinal rocks; the strike-slip faults act as tear faults between crustal blocks that have extended at different times and at different rates. Crustal extension began 13.4–13.1 Ma and migrated northwestward with time; undeformed basalt flows and lacustrine deposits suggest that extension stopped in this region (but continued north of the Death Valley graben) between 5 and 7 Ma. Estimates of crustal extension in this region vary from 30–50 percent to more than 100 percent.

Magmatic rocks syntectonic with crustal extension in the southern Death Valley region include 12.4–6.4 Ma granitic rocks as well as bimodal 14.0–4.0 Ma volcanic rocks. Geochemical and isotopic evidence suggest that the granitic rocks get younger and less alkalic from south to north; the volcanic rocks become more mafic with less evidence of crustal interaction as they get younger.

The close spatial and temporal relation between crustal extension and magmatism suggest a genetic and probably a dynamic relation between these geologic processes. We propose a tectonic-magmatic model that requires heat be transported into the crust by mantle-derived mafic magmas. These magmas pond at lithologic or rheologic boundaries, begin to crystallize, and partially melt the surrounding crustal rocks. With time, the thermally weakened crust is extended (given a regional extensional stress field) concurrent with granitic magmatism and bimodal volcanism.

INTRODUCTION

The Death Valley region in southeastern California is one of the youngest regions of large-scale crustal extension within the Basin-Range province. Normal and associated strike-slip faulting accompanied by extensional basin formation began <15 Ma and continues today (Wright et al., 1981; Stewart, 1980). Numerous granitic plutons, dikes, and sills as well as felsic to mafic volcanic fields are synchronous with extension (Calzia and Finnerty, 1984; Wright et al., 1991; Davis and Fleck, 1977). Previous workers have focused on the timing and kinematics of extensional faulting but few have considered the spatial and temporal relations between extension and magmatism in Death Valley. This paper describes late Cenozoic crustal extension and magmatism in the southern Death Valley region and introduces a tectonic-magmatic model that relates these geologic processes in an actively extending orogen.

GEOLOGIC SETTING

The southern Death Valley region is bounded on the west by the Panamint Range and the south by the Providence Mountains and New York Mountains (Fig. 1). The pre-Cenozoic stratigraphy in this region consists of Early Proterozoic cratonic rocks and Middle Proterozoic to Paleozoic sedimentary deposits. The cratonic rocks include Early Proterozoic paragneiss, schist, and quartzite intruded by ca.1700 Ma orthogneiss and 1400 Ma anorogenic granites (Wooden and Miller, 1990;
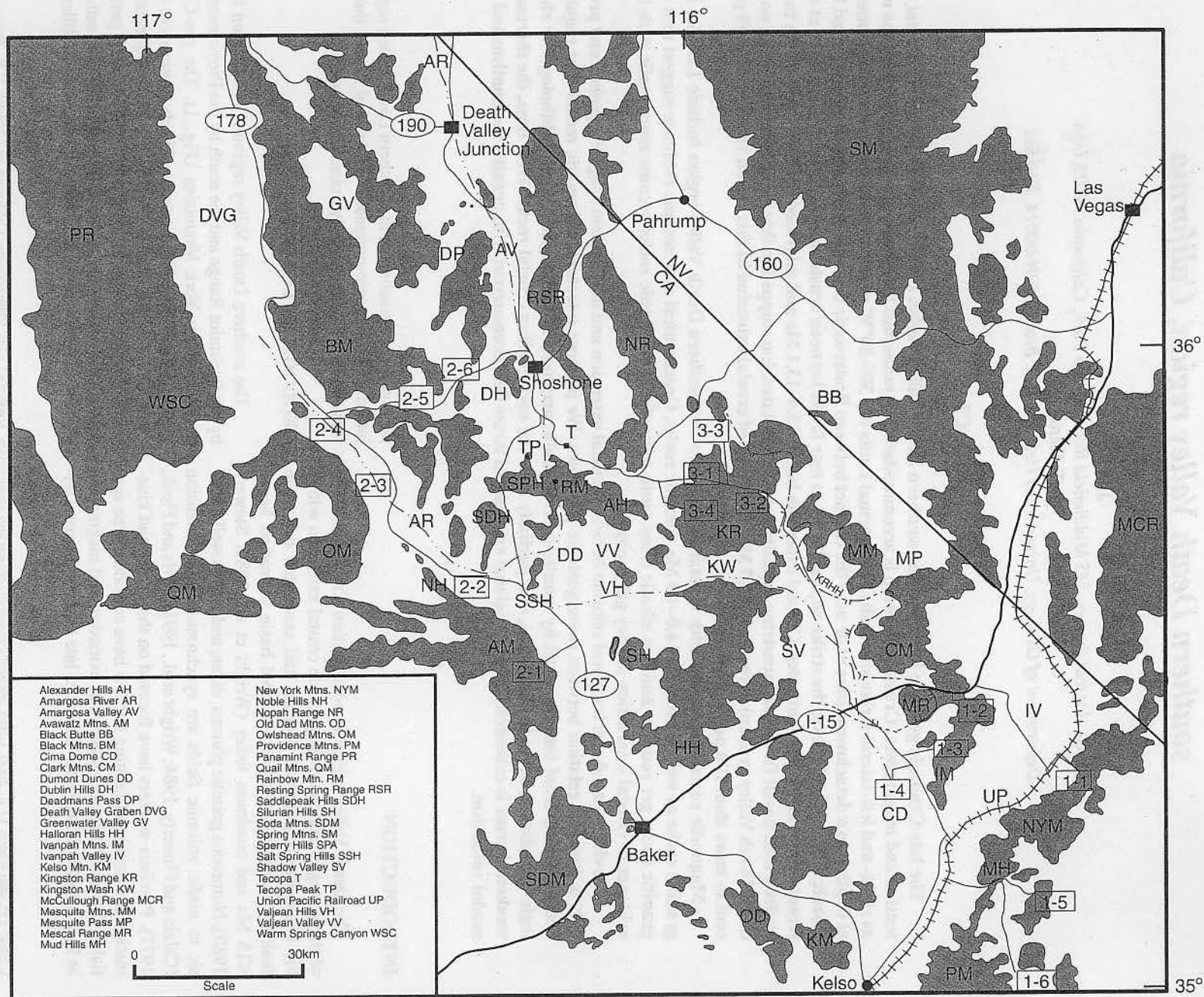
Figure 1A. Index map of the southern Death Valley region showing the Kingston Range-Halloran Hills detachment fault (KRHH), geographic features referred to in the text, major highways, and field trip stops.
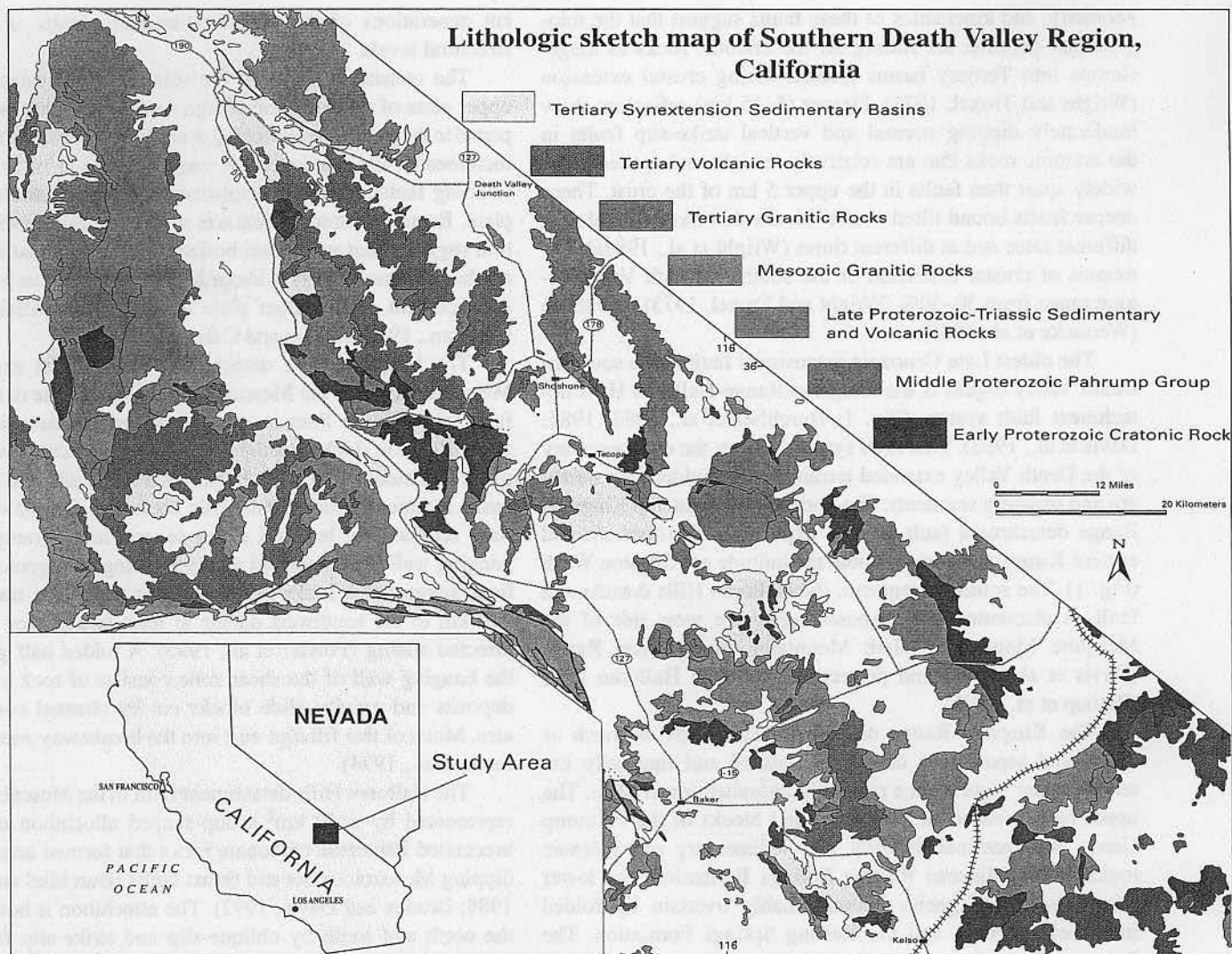
Figure 1B. Lithologic sketch map of the same area shown in Figure 1A.

Lanphere et al., 1964; Rämö and Calzia, 1998). The Middle Proterozoic Pahrump Group unconformably overlies the cratonic rocks and consists of ~2100 m of conglomerate, sandstone, shale, and carbonate rocks divided into the Crystal Spring Formation, Beck Spring Dolomite, and Kingston Peak Formation (Hewett, 1940). The Crystal Spring Formation is intruded by 1068 Ma and 1087 Ma (Heaman and Grotzinger, 1992) diabase sills (Wright, 1968; Hammond, 1986). The Pahrump Group is overlain by 3000–5000 m of Late Proterozoic and Paleozoic miogeoclinal deposits. Most of the Proterozoic and Paleozoic rocks are intruded by Mesozoic and Tertiary plutons (Calzia, 1990; Rämö et al., 2000). All of these rocks are unconformably overlain by later Tertiary sedimentary and volcanic rocks and Quaternary alluvial deposits (Wright and Troxel, 1973).

CRUSTAL EXTENSION

Southwest and west-northwest–directed crustal extension in the southern Death Valley region is accommodated by north-northeast–trending listric and planar normal faults as well as northwest-trending right-lateral and northeast-trending left-lateral strike-slip faults (Wright et al., 1981). Most of the normal faults dip 50°–30°W near the surface and flatten and merge at depth, forming a detachment zone at or near the contact between the cratonic rocks and miogeoclinal deposits (Wright and Troxel, 1973). COCORP (Consortium for Continental Reflection Profiling) lines across the southern Death Valley region show that most of the normal faults do not extend below a depth of 5 km (Serpa et al., 1986, 1988). The pattern,

geometry, and kinematics of these faults suggest that the mio-geoclinal deposits are sliding off the cratonic rocks as mega-slumps into Tertiary basins formed during crustal extension (Wright and Troxel, 1971). Deeper (5–15 km) reflectors show moderately dipping normal and vertical strike-slip faults in the cratonic rocks that are relatively straight and spaced more widely apart than faults in the upper 5 km of the crust. These deeper faults bound tilted crustal blocks that have extended at different rates and at different times (Wright et al., 1984a). Es-timates of crustal extension of the southern Death Valley re-gion range from 30–50% (Wright and Troxel, 1973) to >100% (Wernicke et al., 1988).

The oldest Late Cenozoic extensional fault in the southern Death Valley region is the Kingston Range-Halloran Hills de-tachment fault system (Fig. 1; Burchfiel et al., 1983, 1985; Davis et al., 1993). This fault system defines the east boundary of the Death Valley extended terrain and is divided into north-ern and southern segments. The northern segment, the Kingston Range detachment fault, is well exposed in the northern and eastern Kingston Range to about the latitude of Kingston Wash (Fig. 1). The southern segment, the Halloran Hills detachment fault, is discontinuously exposed along the west side of the Mesquite Mountains, Clark Mountains, and Mescal Range (Davis et al., 1993) and projects beneath the Halloran Hills (Bishop et al., 1991).

The Kingston Range detachment fault dips as much as 15°W and separates a complexly faulted and internally ex-tended upper plate from a relatively unfaulted lower plate. The upper plate consists of thin slices and blocks of the Pahrump Group, miogeoclinal deposits, and sedimentary and volcanic rocks of the Miocene Resting Springs Formation; the lower plate consists of gneiss unconformably overlain by folded miogeoclinal rocks and the Resting Springs Formation. The Pahrump Group is present only in the upper plate of the detach-ment fault. Burchfiel and Davis (1988) noted that the Pahrump Group was deposited in a fault-bounded basin and sug gested that the Kingston Range detachment fault may have reactivated or closely followed the east boundary fault of this Pre-cambrian basin.

Extensional faults in the upper plate of the Kingston Range detachment fault include northwest-trending planar and listric normal faults as well as northeast-trending steep to nearly vertical strike-slip and oblique-slip faults with a large strike-slip component. The northwest-trending faults dip gen-erally to the southwest and merge into the detachment fault or lateral ramps of the detachment fault in the hanging wall; the northeast-trending faults terminate at the detachment fault. Both sets of upper-plate faults are broadly contemporaneous, although several generations of the northwest-trending faults are visible through structural windows in lateral ramps of the detachment fault. Each generation of faults is bounded above and below by subhorizontal faults that locally merge into the detachment fault. The northeast-trending faults are in-ferred to have operated as tear or transfer faults between differ-ent generations of the northwest-trending faults at different structural levels.

The consistent strike of the tear faults indicates that the upper plate of the Kingston Range detachment fault was trans-ported to the southwest (Burchfiel et al., 1983, 1985). Displacement increases to the southwest as each generation of northwest-trending faults added its displacement to the extending upper plate. Reconstruction of contacts within the miogeoclinal sec-tion suggests that maximum horizontal displacement along the northeasternmost faults is about 1–2 km; cumulative horizontal displacement of the upper plate is ~6 km (Burchfiel, written commun., 1989; Fowler and Calzia, 1999).

The Halloran Hills detachment fault is best exposed in Mesquite Pass and the Mescal Range (Fig. 1). The detachment fault in Mesquite Pass is mapped as an anastamosing shear zone, 10–20 m thick, that dips 20°W. The fault cuts lower Pale-ozoic sandstone, a 13.4 Ma hypabyssal felsic sill, and Miocene basin sediments; lower Paleozoic rocks are faulted over Ter-tiary sedimentary breccias along several lateral ramps in the hanging wall (Friedmann et al., 1994). Regional geologic rela-tions suggest that rocks in the hanging wall were transported 5–9 km to the southwest during at least two phases of west-directed sliding (Fowler et al., 1995). A folded half graben in the hanging wall of the shear zone consists of rock avalanche deposits and gravity glide blocks cut by channel conglomer-ates. Much of this fill dips east into the breakaway zone (Fried-mann et al., 1994).

The Halloran Hills detachment fault in the Mescal Range is represented by a 10 km^2 scoop-shaped allochthon of highly brecciated Paleozoic carbonate rocks that formed across west-dipping Mesozoic strata and thrust faults (Burchfiel and Davis, 1988; Brudos and Davis, 1992). The allochthon is bounded on the north and south by oblique-slip and strike-slip faults, re-spectively, and on the east by a complex breakaway zone of down-to-the-west listric normal faults. Cross cutting relations suggest that the allochthon was displaced horizontally approxi-mately 1.5 km during at least two episodes of faulting. Initially, the breakaway zone dipped <30°–50°W; later, a new breakaway zone cut into the footwall of the allochthon and rotated the ini-tial breakaway zone to its present eastward dip. The extremely brittle character of deformation, the abundance of karst matrix between breccia clasts, and the existence of a 0.5 km^2 pull-apart basin with ~100 m of Cenozoic syn- and posttectonic sedimen-tary breccias indicate that deformation within the allochthon took place at or near the surface during Cenozoic time (Brudos and Davis, 1992).

Cross cutting geologic relations bracket the age of crustal extension in the southern Death Valley region. The Kingston Range detachment fault cuts 16.0 Ma (Friedmann, 1996) ash and is cut (Wright, 1968) and deformed (Calzia et al., 1987) by the 12.4 Ma granite of Kingston Peak; 12.5 Ma syntectonic an-desite flows are present in the upper plate of this detachment fault (Calzia, 1990). The Halloran Hills detachment fault cuts a 13.4 Ma felsic sill; 13.1 Ma volcanic breccia was deposited on

the subsiding hanging wall of this fault (Friedmann et al., 1996). A low-angle fault associated with the Halloran Hills detachment fault cuts 13.2 ± 0.4 Ma latite in the northeastern Silurian Hills (Calzia, unpub. data, 1985). Subhorizontal basalt flows and the undeformed Tecopa lake beds unconformably overlie east-tilted strata related to crustal extension in the southern Death Valley region. The basalt flows yield K-Ar ages of 4.48 Ma (Dohrenwend et al., 1984) and 5.12 Ma (Turrin et al., 1985); tuff 17 m above the base of the lake beds (at the present level of erosion) correlates with the 2.02 Ma Huckleberry Ridge Tuff (Hillhouse, 1987). High resolution seismic reflection data indicate, however, that the lake sediments are 134 ± 20 m thick beneath the tuff (Louie et al., 1992). Based on extrapolated sedimentation rates, Louie et al. concluded that the Tecopa lake beds might date back to 7 Ma. These data indicate that large-scale crustal extension in the southern Death Valley region began south of the Kingston Range but north of the Mescal Range and Silurian Hills between 13.4 and 13.1 Ma and migrated northward with time. Extension stopped in this region between 5 and 7 Ma but continues west and north of the Death Valley graben to the present day.

EXTENSIONAL BASINS

The Shadow and Valjean Valleys (Fig. 1) are present-day topographic expressions of two late Cenozoic extensional basins in the southern Death Valley region. These extensional basins are named the Shadow Valley and China Ranch basins. Friedmann and Burbank (1992) reported that the Shadow Valley basin of Hewett (1956) is a supradetachment basin formed in the hanging wall of the Halloran Hills detachment fault. The Shadow Valley basin covers >2500 km^2 and includes 2.5–3.0 km of middle to late Miocene strata deposited during and as a consequence of regional extension. These strata unconformably overlie 19.1 Ma tuff and ~50 m of lacustrine and fluvial sediments in the northern Halloran Hills (Reynolds, written commun., 1984). A pyroxene andesite is interbedded with sediments in the Halloran Hills (Johnson, written commun., 1984); this andesite may correlate with 12.9 ± 0.4 Ma pyroxene andesite in the northern Cima Dome area (Fig. 1; Wilshire, written commun., 1985).

Fill within the Shadow Valley basin is divided into four members separated by regional unconformities that can be linked to basin-wide deformation (Friedmann et al., 1994). Member I consists of carbonate-rich fanglomerate deposits, megabreccias of carbonate rocks and quartzite, volcanic rocks, and minor interbedded lacustrine limestone and siltstone. The volcanic rocks include lahars, basalt to andesite flows, and volcanic breccia. Member II consists of fanglomerate deposits that interfinger with lacustrine sediments and rare volcanic ash. Rock avalanche breccias and gravity glide blocks are common. The fanglomerate deposits coarsen upsection into an alluvial fan complex. Member III consists of fluvial sandstone and con-

glomerate, lacustrine mudstone, and conglomerate of volcanic clasts and the first erosional clasts of the granite of Kingston Peak. Very large gravity glide blocks of gneiss, diabase, and miogeoclinal rocks mapped and photographed by Hewett (1956) are present near the top of this member. Member IV consists of east-tilted cobble to boulder fan deposits; the dip of these fan deposits decreases upsection. Volcanic breccia at the base of Member I and volcanic ash at the base of Member III (the highest volcanic ash in the Shadow Valley basin) yield $^{40}Ar/^{39}Ar$ ages of 13.1 Ma and 10.8 Ma, respectively (Friedmann et al., 1996). Andesite tuff breccia interbedded within a glide block of Paleozoic carbonate rock in Member II yields K-Ar whole-rock and biotite ages of 12.5 ± 0.04 Ma and 12.3 ± 0.04 Ma, respectively (Calzia, unpub. data, 1993).

Northeast- and northwest-trending normal faults cut all four members of the Shadow Valley Basin, repeating basin strata and basal unconformities at least five times across the northern Halloran Hills (Fowler et al., 1995). These faults dip 45°–75°W and have 0.5–3.5 km of displacement; domino-style rotation along the larger faults has produced the 15°–25° eastward tilting of the Shadow Valley basin strata. The larger faults offset Members I-III; Member IV generally overlies the larger faults and is cut by normal faults with displacement <1 km. All four members and most of the normal faults are folded about gently east-plunging axes. The youngest Member IV strata unconformably overlie folded strata south of Kingston Wash. These relations indicate that the folding partially overlapped but also continued after normal faulting (Fowler et al., 1995).

Landslide breccias of Paleozoic carbonate rocks are present around the margin of the Shadow Valley basin at Black Butte, Valjean Hills, and the south end of the Salt Spring Hills as well as in the Silurian Hills (Fig. 1). Landslide breccias at Black Butte consists of brecciated limestone and dolomite from the Cambrian Bonanza King Formation, Anchor and Dawn members of the Devonian Sultan Limestone, and Mississippian Monte Cristo Formation tectonically interbedded with Tertiary volcanic rocks. All of the Paleozoic rocks are overturned and tectonically overlie deformed Tertiary sediments, lacustrine deposits, and volcanic rocks of the Resting Springs Formation; the orientation of faults suggest that the landslide breccias were transported to the southwest. Volcanic rocks interbedded with the limestone and dolomite landslide breccias (shortened here to carbonate breccias) yield K-Ar ages of 12.2–14.0 Ma (Fleck, written commun., 1988); biotite from tuff tectonically overlain by the Sultan Limestone yields a K-Ar age of 12.8 ± 0.3 Ma (Hambrick, written commun., 1988). Biotite from a latite flow interbedded with the Tertiary sediments beneath the carbonate breccias yields a K-Ar age of 13.8 ± 0.3. These data indicate that the carbonate breccias were emplaced after 13.8 Ma and involved rocks as young as 12.2 Ma.

Carbonate breccias in the Valjean Hills include brecciated clasts and blocks of the Bonanza King Formation and black limestone believed to be the Anchor member of the Sultan

Limestone in a comminuted matrix of carbonate rock; the breccias are interbedded with Tertiary lacustrine deposits. Imbrication of the carbonate breccias suggests that they were transported to the southwest. The carbonate breccias tectonically overlie undeformed clastic rocks of the Proterozoic Kingston Peak, Ibex, and Johnnie Formations (Hessler and Friend, 1986).

Carbonate breccias at the south end of the Salt Spring Hills consist of allochthonous blocks of brecciated Bonanza King Formation, Sultan Limestone, and Bird Spring Formation tectonically overlying Cambrian sedimentary rocks, including parautochthonous Bonanza King Formation, and Tetiary volcanic rocks. Bedding within the allochthonous Paleozoic rocks is vertical; Tertiary lacustrine deposits are tectonically interleaved and unconformably overlie these rocks. Limestone breccia mapped as the Sultan Limestone contains Late Silurian to Devonian fossils (Brady, personal commun., 1992); basaltic andesite beneath the carbonate breccias yield a whole-rock K-Ar age of 12.8 ± 0.3 Ma (Calzia, unpub. data, 1994).

Carbonate breccia in the Silurian Hills consists of medium- to coarse-grained recrystallized limestone and dolomite cemented in a matrix of its own debris (Kupfer, 1960); Kupfer named this carbonate breccia the Riggs Formation. The Riggs Formation tectonically overlies gneiss, the Pahrump Group, and miogeoclinal rocks and is unconformably overlain by Tertiary sedimentary and volcanic rocks. Although no fossils have been found, the Riggs Formation is intruded by quartz monzonite porphyry (Kupfer, 1960) that yields K-Ar ages of 88.5–97.2 Ma (Abbott, 1971). Kupfer suggested that the Riggs Formation correlates with Carboniferous carbonate rocks in adjacent ranges; A.R. Prave (written commun., 1995) reported that the Riggs Formation includes carbonate rocks from the Crystal Spring Formation and Beck Spring Dolomite. Calzia (unpub. mapping, 1992) discovered that the Riggs Formation also includes the Bird Spring Formation in the southwestern Silurian Hills. These data suggest that the Riggs Formation is a collection of different carbonate rocks that has been assembled by tectonic processes that predate other late Cenozoic carbonate breccias in the southern Death Valley region.

Except for the Riggs Formation, all of the carbonate breccias at Black Butte and in Valjean Valley consist of the Bonanza King Formation, Sultan Limestone, and Bird Spring Formation. The closest autochthonous outcrops of these rocks are in the Nopah Range and Spring Mountains (Fig 1). The Nopah Range, however, includes a thick section of Paleozoic quartzite where the Spring Mountains do not. None of the carbonate breccias include quartzite. These observations suggest that the carbonate breccias were derived from the Spring Mountains. If so, then minimum run out of these landslide breccias is 63 km to the southwest. Also, if the carbonate breccias originated in the Spring Mountains, then the landslides would have to have gone over the Kingston Range and Kingston Peak at an elevation of 2233 m or the Kingston Range was not there. The carbonate breccias did not originate in the Kingston Range; stratigraphic relations indicate that all post-Cambrian miogeoclinal rocks

were eroded prior to deposition of 16 Ma ash interbedded with fanglomerate and lacustrine deposits in the northern Kingston Range (Calzia, 1990). Regional geologic and geochronological data suggest that the granite of Kingston Peak was exhumed and shedding debris into the Shadow Valley and China Ranch basins between 9.8 Ma and 8.4 Ma (Calzia, 1990; Friedmann et al, 1996). The absence of granite breccia, combined with this geochronological data, suggest that the carbonate breccias are younger than 12.8 Ma but older than 8.4 Ma. They may be temporal equivalents of the large gravity glide blocks of gneiss in Member III of the Shadow Valley basin.

The China Ranch basin is a east-tilted extensional basin, 27 km long by 13 km wide, along the north side of Valjean Valley (Fig. 1); it includes the Sperry Hills basin of Topping (1993) and Dumont Hills basin of Prave and McMackin (1999). The China Ranch basin is filled with volcanic and sedimentary rocks, named the China Ranch beds by Mason (1948), that are approximately the same age as Members III and IV of the Shadow Valley Basin. The China Ranch beds are folded and faulted, so their thickness is not known; estimates vary from as little as 500 m (McMackin, 1997) to 2.0 km (Topping, 1993).

The China Ranch beds unconformably overlie a chaotic assemblage of Middle and Late Proterozoic rocks on Rainbow Mountain and southeast of Tecopa; Late Proterozoic and Paleozoic miogeoclinal rocks are also present beneath China Ranch beds at Tecopa Peak (Fig. 1). The chaotic assemblage on Rainbow Mountain consists of thrust slices of Crystal Spring Formation, Beck Spring Dolomite, Noonday Dolomite, and Johnnie Formation tectonically interbedded with Tertiary fanglomerate, lacustrine, and granitic rocks (Noble, 1941). Individual blocks within the chaos vary from a few meters to 2 km long and up to 300 m thick. Noble correlated this chaotic assemblage with the Jubilee phase of the Amargosa chaos; Wright (1955) reported, however, that Rainbow Mountain is bedrock exposed by faulting during deposition of the China Ranch beds. He concluded that the chaos represents accumulations of sedimentary breccia derived from steep fault scarps. The abundance of cross cutting depositional contacts as well as similarity of structural style indicate that the chaos at Rainbow Mountain is older than the China Ranch beds and is part of the Amargosa chaos; the Middle and Late Proterozoic rocks on Rainbow Mountain are allochthonous and are not bedrock.

A chaotic assemblage of Late Proterozoic rocks is tectonically mixed with Tertiary rocks in low hills 3 km southeast of Tecopa (Fig. 1). This assemblage consists of fault-bounded blocks of Crystal Spring Formation, Beck Spring Dolomite, Noonday Dolomite, Johnnie Formation, and Stirling Quartzite tectonically interbedded with Tertiary lacustrine deposits. Although Tertiary granitic rocks are absent, similar stratigraphic position and structural style suggest that these rocks are also part of the Amargosa chaos and are therefore allochthonous.

Miogeoclinal rocks at Tecopa Peak form an east-dipping homocline of the Stirling Quartzite as well as the Cambrian Wood Canyon Formation and Zabriskie Quartzite. Although

Noble (1941) also considered this homoclinal sequence part of the Jubilee phase of the Amargosa chaos, recent mapping indicates that the structural style of the rocks at Tecopa Peak and within the Amargosa chaos are different. At present, we believe Tecopa Peak is a parautochthonous block of miogeoclinal rocks until geologic or geophysical evidence proves otherwise.

The China Ranch beds consist of dacite overlain by fanglomerate and lacustrine deposits. Highly altered dacite unconformably overlies Amargosa chaos on the south and east side of Rainbow Mountain and yields a K-Ar age of 10.3 Ma (Scott, 1985). Prave and McMackin (1999) divided the overlying fanglomerate deposits into two sequences separated by the lacustrine deposits; the fanglomerate deposits record the unroofing of the granite of Kingston Peak (Topping, 1993). The older fanglomerate sequence is present west of the Amargosa River (Fig. 1) and consists of two east-derived conglomerates that are interbedded with tuff, megabreccia, and landslide deposits (Holm et al., 1994). The older conglomerate consists of clasts derived from the Johnnie Formation and Stirling Quartzite. Lenticular sheets of megabreccia, up to several kilometers long and tens of meters thick, are interbedded with the conglomerate. The megabreccia consists of angular blocks of the Pahrump Group, Johnnie Formation, and Stirling Quartzite that fit together like a giant jigsaw puzzle. Laminated tuff near the base of the older conglomerate but above the lowest megabreccia sheet yields a $^{40}Ar/^{30}Ar$ age of 9.8 Ma (Scott et al., 1988).

The younger conglomerate unconformably overlies the older conglomerate and consists of subangular to rounded clasts of the Pahrump Group, Late Proterozoic miogeoclinal deposits, and Tertiary magmatic rocks including 12–14 Ma latite and the granite of Kingston Peak. This conglomerate includes at least three landslide deposits locally separated by partially welded tuff and algal limestone; the limestone is overlain by 100 m of conglomerate and one last landslide deposit (Holm et al., 1994). The unconformity between the older and younger conglomerates always occurs above the 9.8 Ma tuff and below the first landslide deposit (Holm et al., 1994).

The landslide deposits consist of brecciated blocks of the granite of Ibex Pass and the Crystal Spring Formation interbedded with the conglomerate deposits. The brecciated blocks increase in size from less than 1 km long and a few meters wide near the Amargosa River to several kilometers long and tens of meters high near Highway 127 (Fig. 1). Locally, the deposits are stacked one above the other; successive landslides are separated by subhorizontal shear zones 1–2 m wide.

The fine- to medium-grained granite of Ibex Pass includes feldspar phenocrysts and is characterized by rapakivi textures; biotite from this granite yields a K-Ar age of 12.6 ± 0.3 Ma (Calzia, unpub. data, 1986). Calzia et al. (1990, 1991) concluded that the granite of Ibex Pass is modally, chemically, and isotopically equivalent to the 12.4 Ma granite of Kingston Peak in the Kingston Range 20 km east of the Sperry Hills (Fig. 1).

The genesis of the granite of Ibex Pass has been controversial since Burchfiel et al. (1985) suggested that granitic rocks in the Sperry Hills once might have rested on the granite of Kingston Peak. The granite of Ibex Pass has no intrusive contacts; it tectonically overlies miogeoclinal rocks south of Tecopa Peak, volcanic breccia in the Ibex Pass volcanic field, and younger conglomerates in the older fanglomerate sequence of the China Ranch beds (Fig. 2). Isostatic gravity data indicate that the granite forms a tabular body ~1 km thick and is rootless (Calzia et al., 1991). Although L.A. Wright (written commun., 1993) and McMackin (1997) reported that the granite is autochthonous bedrock, the geologic and geophysical data indicate that it is allochthonous (Calzia et al., 1986; 1991). These data, combined with chemical, isotopic, and geochronological data, support Burchfiel et al. hypothesis, as refined by Topping (1993) and Holm et al. (1994), and suggest that the granite of Ibex Pass is a landslide deposit derived from the granite of Kingston Peak.

The older fanglomerate sequence grades laterally into lacustrine deposits on the south and east side of Rainbow Mountain. The lacustrine deposits are at least 600 m thick and consist of well-bedded sandstone, mudstone, gypsum, and limestone; tuff beds are common and often traceable from the older fanglomerate sequence into lacustrine deposits and the younger fanglomerate sequence.

Scott (1985) and Prave and McMackin (1999) divided the lacustrine deposits into three lithofacies. The oldest lithofacies consists of several fining- and thinning-upward cycles of poorly sorted and cross-bedded sandstone around the margin of the lacustrine deposits. Lenses and channels of pebbly sandstone and conglomerate mark the base of each cycle; laterally persistent limestone beds are common. The sandstone lithofacies is overlain by finer grained cross-bedded sandstone interbedded with mudstone. The finer grained sandstone is cross bedded and characterized by ripple marks; the mudstone becomes more common upsection and contains gypsum, caliche nodules, and root traces. The youngest lithofacies consists of thin-bedded limestone interbedded with mudstone. The limestone contains abundant root casts and molds; the mudstone is characterized by desiccation cracks and mammal tracks. Gypsum is absent in the upper mudstone. Prave and McMackin (1999) concluded that the stratigraphy of the three lithofacies records the change from alluvial fan to fluvial and lacustrine environments.

Tuff beds occur in the upper two lithofacies of the lacustrine deposits. The lowest tuff consists of rounded pumice clasts, biotite flakes, and glass shards. These beds are 2–20 cm thick and are interbedded with mudstone and gypsum. The youngest tuff consists of pumice clasts, is less than 1 m thick, and is interbedded with mudstone. The thickest tuff bed is overlain by siliceous limestone between the middle and upper lithofacies; together, this tuff and limestone define a marker bed within the lacustrine deposits. The tuff is cross laminated, includes pumice clasts and glass shards, and is 2 m thick; it yields a $^{40}Ar/^{39}Ar$ age of 8.4 Ma (Scott et al, 1988) and is correlated with 7.6–8.4 Ma tuff in southwestern California (Sarna-Wojcicki, written commun., 1986).
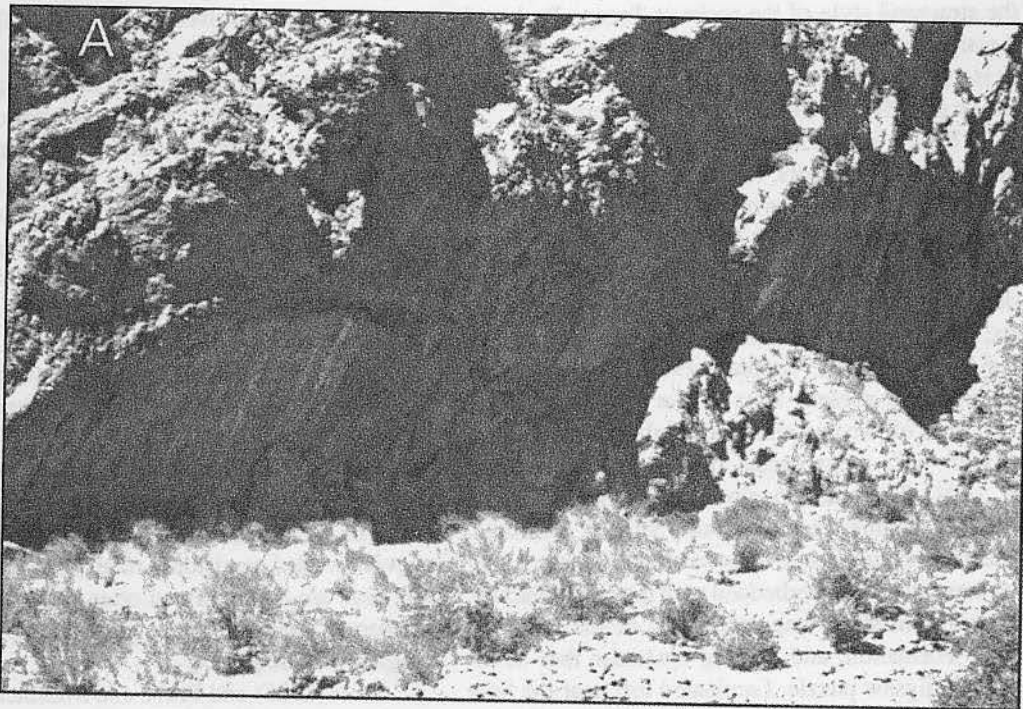
Figure 2. A) Fault contact between landslide breccia of the granite of Ibex Pass and older fanglomerate sequence of the China Ranch beds. B) Detail of the fault breccia and fanglomerate deposit in lower right of photo A. Hammer handle in lower right corner for scale.

The lacustrine deposits grade laterally and vertically into the younger fanglomerate sequence. This fanglomerate sequence occurs east of the Amargosa River and is folded about north- and northeast-trending axes (Wright, 1954). It consists of subrounded to subangular cobbles and boulders of Tertiary volcanic rocks, the granite of Kingston Peak, and the Pahrump Group; paleocurrent data suggests that these clasts were derived from east and west sources (Prave and McMackin, 1999). Large boulders of the granite of Kingston Peak, as large as 10 m across, and monolithologic megabreccia sheets of Pahrump Group rocks are common in the younger fanglomerate sequence (Wright, 1954).

The younger fanglomerate sequence unconformably overlies or is faulted against Proterozoic sedimentary rocks in the Alexander Hills (Fig. 1) and unconformably overlies landslide breccias in Valjean Valley. One landslide breccia, consisting of brecciated blocks of the Beck Spring Dolomite and Kingston Peak Formation tectonically interbedded with Tertiary lacustrine deposits and volcanic breccia, is present just east of the Amargosa River and north of the Dumont Dunes (Fig. 1). A second landslide breccia, consisting of Pahrump Group rocks, diabase, granite of Kingston Peak, and tuff, is overlain by a large slump of the younger fanglomerate sequence southeast of the Alexander Hills and north of the Valjean Hills (Fig. 1). A prominent tuff bed within this slump consists of pumice and glass shards and is correlated with 7.7–8.2 Ma tuff from southern Nevada (Sarna-Wojcicki, written commun., 1998). This tephrochronology data indicate that the prominent tuff bed in the slump block is equivalent to the 8.4 Ma tuff marker bed in the lacustrine deposits, and that slumping of the younger fanglomerate sequence is younger than 8.4 Ma.

The China Ranch beds are unconformably overlain by undeformed alluvial fan and lacustrine deposits in the Tecopa basin. The alluvial fan deposits consist of subequal proportions of clasts derived from the Pahrump Group and mid-Tertiary igneous rocks. Prave and McMackin (1999) concluded that these deposits were derived from cannibalization and reworking of the China Ranch beds or the mixing of alluvial fans derived from local sources.

The lacustrine deposits, locally known as the Tecopa lake beds, are more than 72 m thick and consist of well-bedded mudstone and tufa; four tuffs are interbedded with the mudstone (Hillhouse, 1987; Morrison, 1991). The oldest tuff correlates with the 2.02 Ma Huckleberry Ridge tuff of the Yellowstone Group (Hillhouse, 1987); the youngest tuff is within several meters of the top of the lacustrine deposits and was deposited approximately 160 ka (Morrison, 1991). A third tuff, ~25 m below the youngest tuff, correlates with the 0.62 Ma Lava Creek B ash of the Lava Creek Tuff of the Yellowstone Group; this tuff is locally interbedded with undeformed Quaternary alluvial deposits south of Tecopa (Hillhouse, 1987).

MAGMATISM

Magmatic rocks coeval with Late Cenozoic crustal extension in the southern Death Valley region consist of felsic to mafic plutonic and volcanic rocks in the Kingston Range, Owlshead Mountains, Resting Spring Range, and Black Mountains (Fig. 1). The plutonic rocks can be separated into two petrogenetic suites on the basis of geochronological and chemical data (Calzia and Finnerty, 1984). The older suite yields K-Ar ages of 12–14 Ma and consists of alkalic granites (Fig. 3) characterized by hypabyssal textures, mantled (rapakivi) feldspars, miarolitic cavities, and mafic xenoliths (Calzia, 1990; 1994). The Willow Spring pluton in the central Death Valley volcanic field is the one exception to this grouping. The younger plutonic suite yields K-Ar ages of 10–6.5 Ma and consists of calc-alkalic quartz monzonites with medium- to coarse-grained equigranular and porphyritic textures. Volcanic rocks associated with rapid extension between 14 Ma and 5 Ma are andesitic to felsic in composition; basalts are present but volumetrically insignificant relative to the felsic rocks. Volcanic rocks associated with a relatively slow rate of extension are basaltic in composition and <5 Ma (Asmerom et al., 1994).

Kingston Range

The middle Miocene granite of Kingston Peak and volcanic rocks in the Resting Springs Formation in the Kingston Range are the most extensive magmatic rocks synchronous with the inception of crustal extension in the southern Death Valley region. The granite of Kingston Peak forms an elliptical batholith in the center of the range and is divided into feldspar porphyry, quartz porphyry, and aplite facies based on textural variations and intrusive relations (Calzia, 1990). The feldspar porphyry and quartz porphyry facies, characterized by rapakivi textures and miarolitic cavities, contain mafic xenoliths petrographically and chemically similar to volcanic rocks in the Resting Springs Formation. The aplite facies intrudes and locally is gradational into the feldspar porphyry and quartz porphyry facies. Biotite and hornblende from the feldspar porphyry facies yield concordant K-Ar ages of 12.1 and 12.4 Ma, respectively; incremental heating of chemically homogeneous hornblende from the same sample yields a $^{40}Ar/^{39}Ar$ age of 12.42 Ma (Calzia, 1990).

The granite of Kingston Peak is metaluminuous to slightly peraluminuous and is chemically similar to Cretaceous plutons in the Mesozoic Teutonia Batholith (Calzia, 1990). The feldspar porphyry and quartz porphyry facies yield similar rare earth element (REE) patterns characterized by negative slopes and small negative Eu anomalies; the aplite facies is characterized by lower REE concentrations and by larger negative Eu anomalies. Pb and Sr isotopic data, combined with major and trace element chemical data as well as regional isostatic gravity data, suggest that the feldspar porphyry and quartz porphyry facies were derived by partial melting of Mesozoic batholithic rocks at mid-crustal levels. New Nd isotopic data (Calzia and Rämö, 1997; Rämö et al., 1999) suggest that these batholithic rocks had been hybridized by mantle-derived magmas during the initial stages of Tertiary extension. The aplite facies was derived by complex magmatic processes including crystal fractionation and exsolution of a vapor phase. Stratigraphic reconstruction of Proterozoic, Paleozoic, and Miocene

A

WEIGHT % (Na₂O + K₂O)

$WEIGHT\ \%\ (Na_2O + K_2O)$

12

Alkalic

8

4

Subalkalic

0

55 65 75

$WEIGHT\ \%\ SiO_2$

○ 14.0-4.0 Ma volcanic rocks

○ 12-14 Ma granitic plutons

◌ 10-6.5 Ma granitic plutons

0.2

Calc-alkalic

$FeO\,(tot)/FeO(tot) + MgO$

0.6

1.0

Tholeiitic

B

10

n=64

$FREQUENCY$

0

45 55 65 75

$WEIGHT\ \%\ SiO_2$
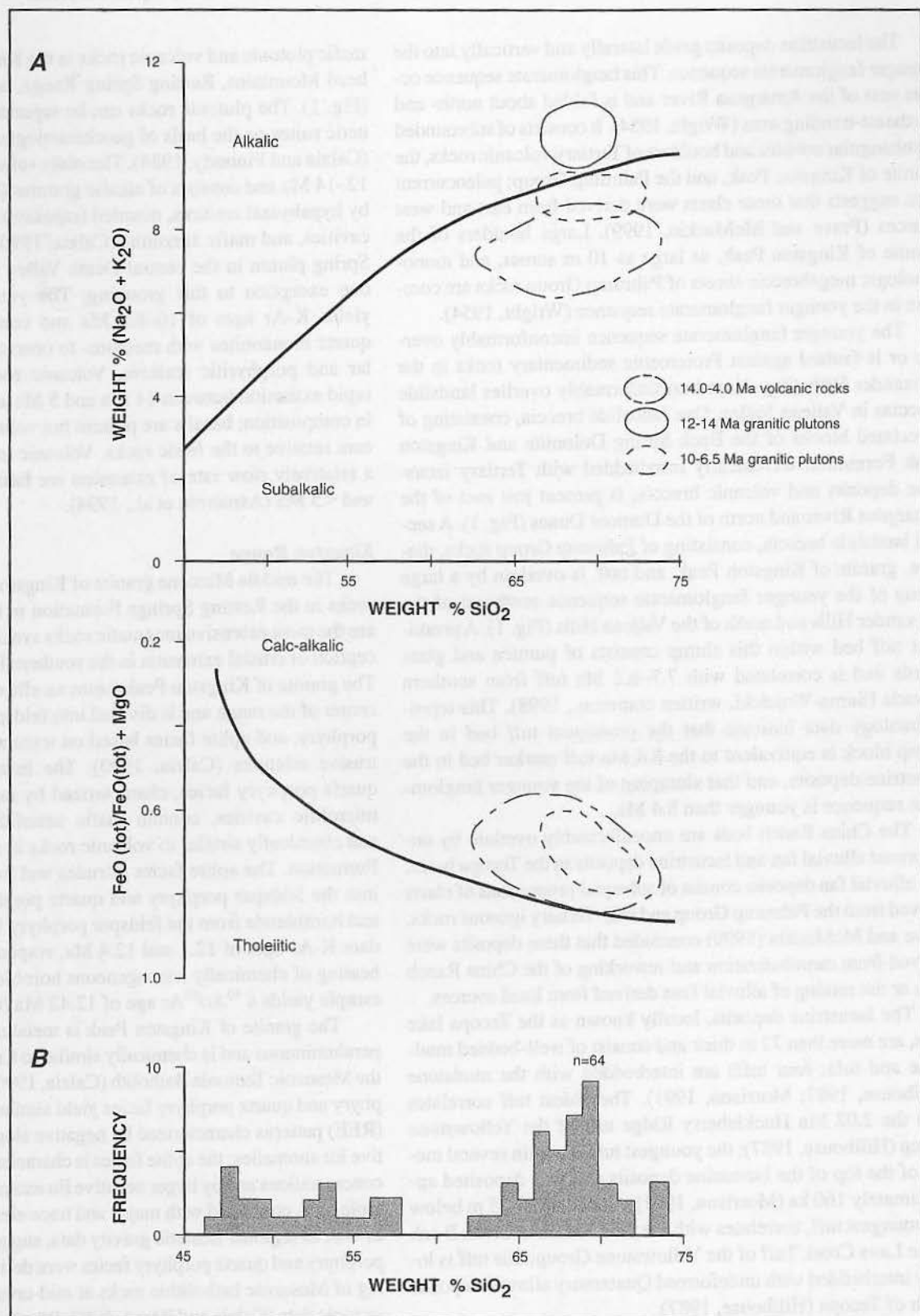
Figure 3. Geochemistry of late Cenozoic magmatic rocks in the southern Death Valley region. A) Chemical classification of magmatic rocks (Irvine and Baragar, 1971; Miyashiro, 1974). B) Wt% SiO₂ of volcanic rocks in the southern Death Valley region.

country rocks indicates that the granitic melt was emplaced at shallow (~4 km) crustal levels (Calzia, 1990).

Volcanic rocks in the Resting Springs Formation consist of porphyritic andesite flows, interbedded with rare basalt lenses and white lithic tuff, unconformably overlain by volcanic breccia of andesite, basalt, and latite cobbles in a matrix of calcareous tuff (Calzia, 1990). A well-developed magmatic foliation, expressed by plagioclase phenocrysts as large as 4 mm, occurs in andesite flows in the north half of the range and in Kingston Wash. It is not known whether this texture was originally limited to a single flow of regional extent, or to multiple flows with similar cooling histories, because the rock is too badly altered for a reliable chemical fingerprint. Biotite from andesite flows in the north half of the range yield K-Ar ages of 12.1 Ma (Calzia, 1991) and 12.5 Ma (Spencer, written commun., 1981).

Volcanic rocks in the Resting Springs Formation and mafic xenoliths in the granite of Kingston Peak are alkalic and calc-alkalic (Fig. 3) and contain 7%–11% total alkalis (Calzia, 1990). Chondrite-normalized REE patterns of these rocks are characterized by steep negative slopes and the lack of an Eu anomaly. Trace element data as well as Sr and Nd isotopic data suggest that the volcanic rocks and mafic xenoliths crystallized from mafic magmas produced by partial melting of lithospheric mantle. These source rocks are characterized by high Sr concentrations and $^{87}Sr/^{86}Sr$ ratios as well as negative ε_{Nd} values (Calzia, 1990; Calzia and Rämö, 1997).

Steep linear patterns on Pb isotopic plots, at acute angles to 1700 and 100 Ma reference isochrons, suggest that the granite of Kingston Peak, volcanic rocks in the Resting Springs Formation, and mafic xenoliths in the granite are cogenetic (Calzia, 1990). Although the mafic xenoliths have comingled with the granite, nonlinear major- and trace-element variation diagrams as well as Sr isotopic data preclude extensive magma mixing between these rocks. Anomalous Na_2O and Rb concentrations and high Pb isotopic ratios indicate that the mafic melts assimilated crustal material at some time in their magmatic history. Combined, the geologic, geochemical, and isotopic data suggest that mantle-derived mafic magmas, represented by the volcanic rocks in the Resting Springs Formation, have partially melted Mesozoic batholithic rocks at mid-crustal levels to produce the granite of Kingston Peak (Calzia, 1990).

Cross cutting geologic relations and petrographic data indicate that the granite of Kingston Peak and volcanic rocks in the Resting Springs Formation are syntectonic with crustal extension. The granite cuts the Kingston Range detachment fault and is cut by listric normal faults along the west side of the range (Calzia et al., 1987). Rhyolite porphyry dikes locally fill the projected trace of the detachment fault (Wright, 1968) and are cut by the listric faults (Calzia, 1990). Regional isostatic gravity and paleomagnetic data suggest that the granite also is cut by another detachment fault at depth and tilted about 30°NE (Calzia et al., 1986; Fowler and Calzia, 1999). The abundance of strained quartz crystals as well as fractured and brecciated quartz and feldspar crystals healed by quartz and opaque oxides suggest that the granite was emplaced and crystallized in an active tectonic environment. Combined, the geologic and petrographic data indicate that the granite of Kingston Peak postdates the Kingston Range detachment fault but predates another flat fault at depth. The granite is extended by listric normal and strike-slip faults that are synchronous with Late Cenozoic crustal extension in the southern Death Valley region.

Ibex Pass

The Ibex Pass volcanic field consists of volcanic flows and rhyodacite stocks in the Sperry and Saddlepeak Hills (Fig. 1; Troxel and Calzia, 1994). The volcanic flows unconformably overlie Late Proterozoic miogeoclinal rocks and consist of olivine basalt, porphyritic andesite, and rhyodacite flows overlain by porphyritic tuff; rhyodacite stocks intrude the Kingston Peak Formation in the northern Saddlepeak Hills and are similar in composition to the rhyodacite flows. All of these rocks are overlain by volcanic breccia, characterized by rounded to subangular cobbles of andesite, basalt, and tuff in an andesite matrix; that is tectonically overlain by landslide deposits of granite in the China Ranch basin. A chaotic assemblage of the volcanic rocks, Noonday Dolomite, and Tertiary lacustrine deposits is tectonically interbedded with basalt and andesite flows in the southern Sperry Hills. This volcanic chaos resembles landslide breccias in the Shadow Valley and China Ranch basins. Biotite from a rhyodacite flow near the middle of the volcanic sequence yields a K-Ar age of 12.3 ± 0.31 Ma (Calzia, unpub. data, 1986).

Basalt to andesite dikes in the southern Saddlepeak Hills trend N45°W, are nearly vertical, and yield a K-Ar age of 12.7 Ma (Troxel and Calzia, 1994). The dikes fill fractures that are cut by steeply dipping normal faults that merge with a more northerly-trending master fault; the master fault transverses the Saddlepeak Hills and is truncated by a complex system of nearly flat faults along the crest of the range.

Owlshead Mountains

Miocene tuffs as well as volcanic lahars, breccias, and flows unconformably overlie Cretaceous quartz monzonite in the central Owlshead Mountains (Davis and Fleck, 1977). The oldest volcanic rocks consist of 14.1 Ma biotite pumiceous tuff unconformably overlain by a thick section of andesite to basaltic lahars and volcanic breccia. Locally, the tuff unconformably overlies a thin discontinuous wedge of arkosic grit and carbonate debris deposited on the erosional surface of quartz monzonite. The lahars and breccia are separated into upper and lower units by a 13.4 Ma tuff, and are overlain by 12.9 Ma platy pyroxene andesite. The platy andesite is intruded by 12.9 Ma andesite plugs and unconformably overlain by 12.6 Ma olivine basalt (Davis, written commun., 1990).

These volcanic and sedimentary rocks include three sheet-like allochthons that lie discordantly on one another. These gravity-driven allochthons cover >30 km² and have a minimum northeastward displacement of 10 km (Davis and Fleck, 1977). Locally, the allochthons overlie similar authochthonous volcanic rocks and the granitic basement. North-south normal faulting

and erosion preceded emplacement of the lowest (oldest) sheet; a second episode of high-angle northeast-southwest normal faulting and erosion preceded emplacement of the younger allochthons. The 12.9 Ma andesite plugs cut the base of the highest (youngest) sheet. Field and geochronological data indicate that volcanism, high-angle block faulting, and gravity sliding occurred within a 1–2 m.y. period from 14.1 Ma–12.6 Ma; the period from 12 Ma to present is characterized by uplift and doming of the Owlshead Mountains (Calzia, 1974; Brady, 1985, 1990).

A thick section of porphyritic andesite flows in the southern Owlshead Mountains overlies or locally is interbedded with andesitic lahars and breccias in the central Owlshead Mountains. These porphyritic flows dip southwest and overlie 1 m of fanglomerate deposits and 3 m of white tuff in the Quail Mountains (Fig.1; Muehlberger, written commun., 1992). Plagioclase from the porphyritic andesite yields a K-Ar age of 13.1 ± 0.4 Ma (Calzia, unpub. data, 1994). The field and geochronological data suggest that the porphyritic andesite flows correlate with the 12.9 Ma pyroxene andesite in the central Owlshead Mountains.

Wagner (1988) described more than 2000 m of andesitic lahars, breccias, and flows that overlie granite in the Panamint Range north of the Owlshead Mountains. Discontinuous lenses of pumiceous rhyolitic tuff, arkosic grit 0–3 m thick, and conglomerate with granitic boulder clasts locally are present between the volcanic rocks and granite. The rhyolitic tuff thickens toward the west. Johnson (1957) mapped several rhyolite intrusions in the southwestern Panamint Range that may be the source of the rhyolitic tuff.

Wagner (1988, 1994) described an eroded volcanic center between the Owlshead Mountains and Panamint Range. His volcanic center consists of an intrusive complex of basalt, gabbro, and rhyolite plugs, dikes, and volcanic necks partially buried by a volcanic edifice of andesitic to basaltic breccias, flows, and tuffs. Swarms of basalt to latite plugs, dikes, and sills extend from the intrusive complex and cut the volcanic edifice; a basalt plug in the intrusive complex yields a whole rock K-Ar age of 14.0 ± 0.3 Ma (Wright, written commun., 1984). Overlying the intrusive complex are lapilli tuffs and tuff breccia that represent ignimbrites deposited within a crater; flanking the intrusive complex are stratified andesite flows, breccias, and tuff that made up the volcanic cone. Wrucke (1966) reported that pyroxene andesite flows and volcanic breccia in the southern Panamint Range are overlain by olivine basalt and locally interbedded with pumice-rich lapilli tuffs. He estimated the volcanic rocks are more than 1,000 m thick on the south side of Warm Springs Canyon (Fig. 1); hornblende from a flow on the north side of the canyon yields a $^{40}Ar/^{39}Ar$ plateau age of 13.7 Ma (Topping, 1993).

Resting Spring Range

Volcanic rocks in the Resting Spring Range are mapped as part of the Chicago Valley Formation, tuff of Resting Spring Pass, and as isolated outcrops of basalt along the crest of the range. The Chicago Valley Formation is 125–190 m thick and unconformably overlies Cambrian miogeoclinal deposits along the east side of the Resting Spring Range (Wilhelms, 1963; Laibidi, 1981). This formation dips as much as 50°–60°E (nearly as much as the underlying miogeoclinal rocks) and decreases upsection. This variation in dip suggests that deposition of the Chicago Valley Formation was concurrent with tilting of the Resting Spring Range.

The Chicago Valley Formation consists of lower clastic and upper limestone units separated by a volcanic unit. The clastic unit includes a basal conglomerate, consisting of angular fragments of the underlying miogeoclinal rocks as well as exotic clasts of Devonian carbonate rocks, orthoquartzite, and Jurassic leucogabbro (Wernicke, written commun., 1993), overlain by cross-bedded sandstone and sandy limestone. Tuff interbedded with conglomerate in the northern part of the range yields a $^{40}Ar/^{39}Ar$ age of 14.7 Ma (Niemi et al., 1999). The volcanic unit consists of a basal lapilli tuff with andesite, syenite, and rare granitic cobbles overlain by an interbedded sequence of flow-banded basalt and andesite flows and volcanic breccia. The basalt and andesite flows contain plagioclase, augite, and olivine phenocrysts; abundant basalt inclusions and rare sanidine phenocrysts are present in the andesite. Plagioclase phenocrysts locally are parallel to flow banding in the basalt and are characterized by spongy rims in the andesite. The volcanic breccia consists of cobbles and boulders of basalt and andesite with lenses of dolomite breccia near the top of this unit. Biotite from an andesite flow near the top of the volcanic unit yields a K-Ar age of 11.7 ± 0.2 Ma (Wright, written commun., 1984). The abundance of basalt inclusions, sanidine phenocrysts, and partially resorbed plagioclase phenocrysts suggest that the andesite flows were derived by crustal contamination of basaltic magmas that are syntectonic with tilting of the Resting Spring Range.

The tuff of Resting Spring Pass unconformably overlies the Chicago Valley Formation and Gerstley lake beds; it is 60–250 m thick and includes as many as five rhyolitic cooling units (Laibidi, 1981). The base of the thickest cooling unit consists of nonwelded lapilli tuff with pumice and lithic fragments. The nonwelded tuff is overlain by a partially welded zone, characterized by flattened pumice fragments, and a densely welded zone of obsidian and devitrified tuff. The devitrified tuff is characterized by numerous cavities filled with quartz, cristobalite, tridymite, and feldspar. The densely welded zone is overlain by cliff-forming partially welded to nonwelded lapilli tuff with pumice fragments; crystals of plagioclase, sanidine, biotite, quartz, and minor pyroxene are common throughout this zone. The upper partially welded tuff is overlain by nonwelded tuff preserved in a few localities at the top of this formation. Devitrified tuff above the obsidian yields a whole-rock K-Ar age of 9.6 ± 0.1 Ma (Wright, written commun., 1984).

Isolated outcrops of subhorizontal basalt overlie fanglomerate deposits along the crest of the Resting Spring Range. The basalt is as much as 15 m thick and is vesicular and porphyritic; phenocrysts of plagioclase, augite, and olivine are common. Basalt from the southernmost outcrop 8 km north of Resting Spring Pass yields a whole-rock K-Ar age of 9.5 ± 0.1 Ma

(Wright, written commun., 1984). Petrographic and geochronological data suggest that basalt along the crest of the Resting Spring Range is equivalent to 9.3 ± 0.3 Ma basalt in the Dublin Hills and 9.3 ± 0.3 Ma basalt just north of Shoshone (Calzia, unpub. data, 1994). If correct, then uplift and tilting of the Resting Spring Range was complete by 9.5 Ma, and the Amargosa Valley (Fig. 1) formed after 9.3 Ma but before deposition of the Gerstley lake beds; the age of the Gerstley lake beds is uncertain (Barker and Wilson, 1975).

Black Mountains

The central Death Valley volcanic field (CDVVF) in the Black Mountains covers 1300 km² between the right-lateral Furnace Creek fault zone on the north and the left-lateral

(Blakely, written commun., 1992) Sheephead Pass fault zone to the south (Fig. 4; Wright et al., 1981, 1991). The CDVVF consists of late Cenozoic plutonic and volcanic rocks that intrude or overlie a chaotic assemblage of Early Proterozoic gneiss and tectonically attenuated Proterozoic and Cambrian sedimentary rocks. Noble (1941) named this chaotic assemblage the Amargosa chaos and the fault between the chaos and autochthonous gneiss the Amargosa thrust (renamed Amargosa fault by Wright et al., 1991). Locally, the oldest volcanic rocks are cut by numerous arcuate normal faults that dip west, flatten with depth, and merge with the Amargosa fault or with faults within the chaos. Wright et al. (1991) concluded that the CDVVF represents an igneous rhombochasm because it lies between two en echelon strike-slip fault zones and is in part
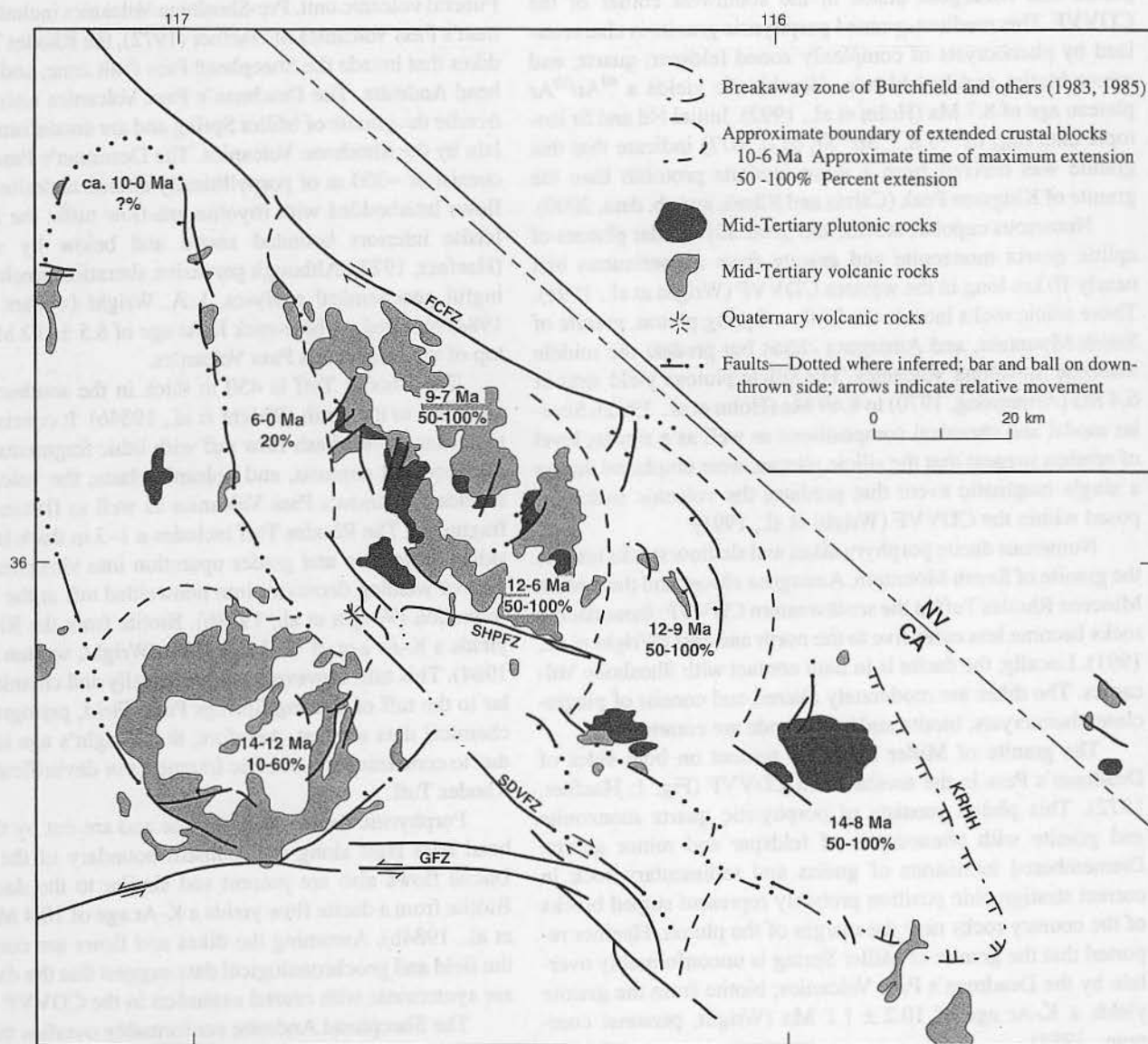
Figure 4. Approximate time and percent extension of crustal blocks in the southern Death Valley region. FCFZ—Furnace Creek fault zone; GFZ—Garlock fault zone; KRHH—Kingston Range–Halloran Hills detachment fault; SDVFZ—Southern Death Valley fault zone; SHPFZ—Sheephead Pass fault zone.

coeval with the Amargosa fault and extensional structures in the Amargosa chaos.

The Willow Spring pluton, the oldest igneous rock in the CDVVF, consists of an elongate sill of fine-grained gabbro and diorite that intrudes gneiss along the west side of the Black Mountains. The gabbro includes nearly equal parts of hornblende and andesine; the diorite is characterized by lesser amounts of hornblende, greater amounts of andesine, and minor amounts of quartz and potassium feldspar (Otton, 1977). The gabbro has a particularly juvenile composition with initial ε_{Nd} of -1 to -2, and $^{87}Sr/^{86}Sr_i$ of 0.706 (Asmerom et al., 1990; Calzia and O.T. Rämö, unpub. data, 2000). Asmerom et al. reported that zircon from the Willow Spring pluton yields a U-Pb age of 11.6 Ma.

The granite of Smith Mountain intrudes the Willow Spring pluton and Amargosa chaos in the southwest corner of the CDVVF. This medium-grained porphyritic granite is characterized by phenocrysts of complexly zoned feldspar, quartz, and minor biotite and hornblende. Hornblende yields a $^{40}Ar/^{39}Ar$ plateau age of 8.7 Ma (Holm et al., 1992). Initial Nd and Sr isotopic data (ε_{Nd} of -5.8, $^{87}Sr/^{86}Sr_i$ of 0.7077) indicate that this granite was derived from a more juvenile protolith than the granite of Kingston Peak (Calzia and Rämö, unpub. data, 2000).

Numerous cupolas, stocks, and generally tabular plutons of aplitic quartz monzonite and granite form a continuous belt nearly 10 km long in the western CDVVF (Wright et al., 1991). These silicic rocks intrude the Willow Spring pluton, granite of Smith Mountain, and Amargosa chaos but predate the middle Miocene Shoshone Volcanics. The silicic plutons yield ages of 6.4 Ma (Armstrong, 1970) to 8.69 Ma (Holm et al., 1992). Similar modal and chemical compositions as well as a similar level of erosion suggest that the silicic plutons were emplaced during a single magmatic event that predates the volcanic rocks exposed within the CDVVF (Wright et al., 1991).

Numerous dacite porphyry dikes and shallow stocks intrude the granite of Smith Mountain, Amargosa chaos, and the middle Miocene Rhodes Tuff in the southwestern CDVVF; these dacitic rocks become less extensive to the north and east (Wright et al., 1991). Locally, the dacite is in fault contact with Shoshone Volcanics. The dikes are moderately altered and consist of plagioclase phenocrysts; biotite and hornblende are common.

The granite of Miller Spring is present on both sides of Deadman's Pass in the southeastern CDVVF (Fig. 1; Haefner, 1972). This pluton consists of porphyritic quartz monzonite and granite with phenocrysts of feldspar and minor quartz. Dismembered inclusions of gneiss and sedimentary rock in correct stratigraphic position probably represent stoped blocks of the country rocks near the margin of the pluton. Haefner reported that the granite of Miller Spring is unconformably overlain by the Deadman's Pass Volcanics; biotite from the granite yields a K-Ar age of 10.2 ± 1.1 Ma (Wright, personal commun., 1984).

The Shoshone pluton in the southeastern CDVVF consists of an outer porphyritic facies of fine- to medium-grained quartz monzonite intruded by an inner aplitic facies. The porphyritic facies is characterized by feldspar phenocrysts up to 10 mm long and rapakivi textures (Novak, 1967); acicular hornblende crystals are common. The groundmass of the porphyritic facies changes from granophyric to aphanitic toward the center of the pluton. Almashoor (1980) concluded that the Shoshone pluton was emplaced at 2.0–2.5 km and is tilted to the east; sedimentary inclusions, similar to those in the granite of Miller Spring, probably represent stoped blocks of the country rocks near the margin of the pluton. The Shoshone pluton is unconformably overlain by the Deadman's Pass and Shoshone volcanics; biotite from the pluton yields a $^{40}Ar/^{39}Ar$ age of 9.8 Ma (Holm et al., 1992).

Volcanic rocks in the CDVVF are divided into the pre-Shoshone, Shoshone, and Greenwater Volcanics as well as the Funeral volcanic unit. Pre-Shoshone Volcanics include the Deadman's Pass Volcanics of Haefner (1972), the Rhodes Tuff, dacite dikes that invade the Sheephead Pass fault zone, and the Sheephead Andesite. The Deadman's Pass Volcanics unconformably overlie the granite of Miller Spring and are unconformably overlain by the Shoshone Volcanics. The Deadman's Pass Volcanics consist of ~300 m of porpyllitically altered andesite and dacite flows interbedded with rhyolite ash-flow tuffs; the flows have felsite interiors bounded above and below by vitrophyres (Haefner, 1972). Although pervasive alteration precludes meaningful geochemical analyses, L.A. Wright (written commun., 1984) reported a whole-rock K-Ar age of 8.5 ± 0.2 Ma from the top of the Deadman's Pass Volcanics.

The Rhodes Tuff is 450 m thick in the southern CDVVF and thins to the north (Wright et al., 1984b). It consists of weak to densely welded ash-flow tuff with lithic fragments of gneiss, miogeoclinal deposits, and volcanic clasts; the volcanic clasts include Deadman's Pass Volcanics as well as flattened pumice fragments. The Rhodes Tuff includes a 1–2 m thick layer of obsidian at its base and grades upsection into vitrophere; the degree of welding decreases into nonwelded tuff at the top of this formation (Wright et al., 1984b). Biotite from the Rhodes Tuff yields a K-Ar age of 10.7 ± 0.4 Ma (Wright, written commun., 1984). This tuff, however, is lithologically and chemically similar to the tuff of Resting Springs Pass. Field, petrographic, and chemical data suggest, therefore, that Wright's age is incorrect due to contamination of lithic fragments or devitrification of the Rhodes Tuff.

Porphyritic dacite dikes intrude and are cut by the Sheephead Pass fault along the southern boundary of the CDVVF. Dacite flows also are present and similar to the dacite dikes. Biotite from a dacite flow yields a K-Ar age of 10.4 Ma (Wright et al., 1984b). Assuming the dikes and flows are comagmatic, the field and geochronological data suggest that the dacite dikes are syntectonic with crustal extension in the CDVVF.

The Sheephead Andesite conformably overlies the Rhodes Tuff, is 210 m thick, and is divided into lower and upper andesite units separated by a middle vocanoclastic unit (Wright et al., 1984b). The lower andesite unit consists of vesicular por-

phyritic andesite flows and flow breccias; the flow-banded upper unit is neither as porphyritic nor as vesicular as the lower unit. The volcanoclastic breccia is 3–10 m thick and consists of volcanic clasts, up to 70 cm in diameter, as well as rare lithic fragments of clastic and carbonate rocks.

The Shoshone Volcanics unconformably overlie the pre-Shoshone Volcanics in the CDVVF. The Shoshone Volcanics are 900 m thick and include dacite and rhyolite tuffs and flows that erupted between 7.5 Ma and 8.5 Ma (Wright et al., 1991). These tuffs and flows are color banded in shades of yellow, brown, and gray resulting in a calico colored landscape.

A typical eruptive unit in the Shoshone Volcanics consists of ash-fall tuff overlain by a rhyolitic flow (Haefner, 1972). The well-stratified tuff is generally <10 m thick and consists of plagioclase phenocrysts, hornblende, and biotite in a devitrified matrix of lapilli tuff. The rhyolitic flow is 30–100 m thick and divided into lower and upper vitrophyre zones separated by a vesicular felsophyre zone. Vitrophyre and felsophyre zones contain plagioclase phenocrysts as well as hornblende and biotite; the vitrophyric groundmass consists of perlitic glass with pyroxene crystallites.

The Greenwater Volcanics are present in a belt ~50 km long along the east side of the CDVVF. These rocks unconformably overlie the Shoshone Volcanics and yield K-Ar ages of 5–7 Ma (Wright et al., 1991). The basal part of the Greenwater Volcanics consists of basalt and andesite flows interbedded with silicic ash-flow tuffs and tuffaceous sediments. These rocks are overlain by massive glassy dacite flows and breccias that grade eastward into flow-dome complexes; these flow-dome complexes probably represent vent areas for the Greenwater Volcanics. The dacite flows and domes are overlain by ash-flow tuffs that locally overlie andesite flows in the northern Greenwater Valley (Fig. 1). Basalt and andesite flows near the base of the section contain olivine, clinopyroxene, plagioclase, and opaque oxide phenocrysts; the dacite flows contain plagioclase, hornblende, biotite, or opaque oxide phenocrysts. Basalt and andesite occur as partially disaggregated inclusions in dacite flows and represent incomplete homogenization of magmas prior to or during eruption of the dacite flows.

The Funeral volcanic unit in the CDVVF include 4.0–4.8 Ma (Wright et al., 1991) basalt and andesite flows and agglomerate in the Funeral Formation, as well as the 4.9 Ma (Otton, 1977) basalt of Copper Canyon. Basalt flows and agglomerate in the Funeral Formation are ~150 m thick; the flows contain olivine, clinopyroxene, and plagioclase phenocrysts in a fine- to medium-grained trachytic groundmass. The agglomerate consists of cinders, scoria, bombs, and breccia and probably represents eroded vents of the basalt. The basalt of Copper Canyon is 350 m thick and is interbedded with conglomerate and sedimentary breccias in the lower and middle sections of the Copper Canyon Formation (Otton, 1977). These rocks are generally subhorizontal or moderately tilted to the east and are synchronous with uplift and erosion of the CDVVF.

TECTONIC-MAGMATIC MODEL

Figure 4 illustrates the northwestward migration of crustal extension and magmatism with time in the southern Death Valley region. Extension began 13.4–13.1 Ma ago with development of the Kingston Range-Halloran Hills detachment fault. This detachment fault was buried by syntectonic sedimentary and volcanic rocks in the Shadow Valley basin and intruded by the 12.4 Ma granite of Kingston Peak in the Kingston Range. Tilting of the Resting Spring Range postdates 11.7 Ma basalt and andesite flows that flank the range, and predates 9.5 Ma basalt along the crest of the range. Older (8.5–7 Ma) dacite and rhyolite flows in the central Death Valley volcanic field dip as much as 60°E whereas younger (5–4 Ma) basalt flows are subhorizontal. This close spatial and temporal relation between crustal extension, granitic magmatism, and volcanism (Fig. 5) suggest a genetic and probably a dynamic relation between these geologic processes. Lucchitta (1985, 1990) proposed that both extension and magmatism are driven by heat. Briefly, heat advected into the crust from mantle-derived basaltic magmas reduces the shear strength and partially melts the crust. The thermally weakened crust is then extended, given a regional extensional stress field, concurrent with granitic magmatism and bimodal volcanism.

The southern Death Valley region has high and variable heat flow with thermal gradients greater than the Basin–Range region and similar to those measured at Battle Mountain, Nevada (Fig. 6; Lachenbruch, personal commun., 1987; Lachenbruch et al., 1985). The most probable source of anomalous heat is upward migration of basaltic magmas that underplate the crust at the Moho or intrude the lower crust and pond at abrupt lithologic, density, or rheologic boundaries (Lachenbruch and Sass, 1977). The basaltic magmas begin to crystallize and exchange heat with the adjacent crustal rocks. If basaltic underplating or intrusion persists, heat advected into the lower crust will establish a thermal front with steep gradients that migrate laterally and vertically with time.

Heat advected into the lower crust tends to focus later intrusions and begins to partially melt crustal rocks (Hildreth, 1981; Glazner and Ussler, 1988; Huppert and Sparks, 1988). Xenolith studies and modeling of seismic data suggest that the lower crust in the southern Death Valley region consists of a heterogeneous mix of mafic- to intermediate-composition igneous sills interlayered with ductily deformed crust characterized by transposed compositional layering (Wilshire et al., 1988; Wilshire, 1990; McCarthy and Thompson, 1988). Assuming a granodiorite (intermediate) composition, the lower crust beneath the southern Death Valley region would begin to melt along the granodiorite water-saturated solidus (GSS) or granodiorite dry solidus (GDS) depending on the presence or absence of excess water (Fig. 6). If water is present, H_2O-saturated melts of rhyolite composition will be generated near the GSS. With continued melting, excess water would be dissolved and
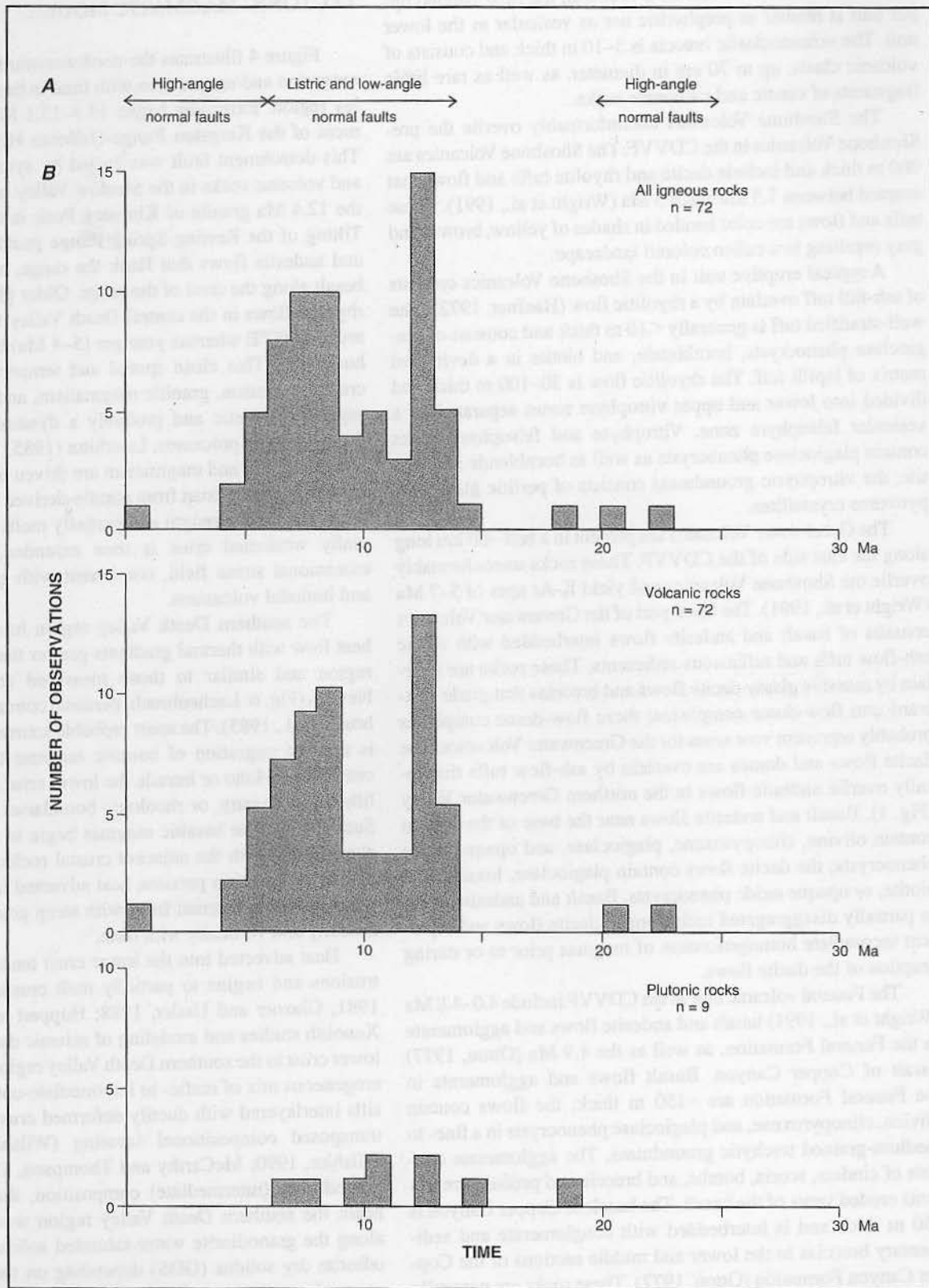
Figure 5. Temporal relation between late Cenozoic crustal extension and magmatism in the southern Death Valley region. A) Periods of crustal extension separated by styles of normal faulting. B) Histograms of K-Ar ages of magmatic rocks.

TEMPERATURE, °C

BM	Characteristic thermal gradients of Battle Mountain, NV.
BR	Characteristic thermal gradients of Basin-Range province
GSS	Granodiorite water-saturated solidus
GDS	Granodiorite dry solidus
BS	Basalt solidus
TB	Depth to base of Teutonia Batholith (ca. 15 Ma)
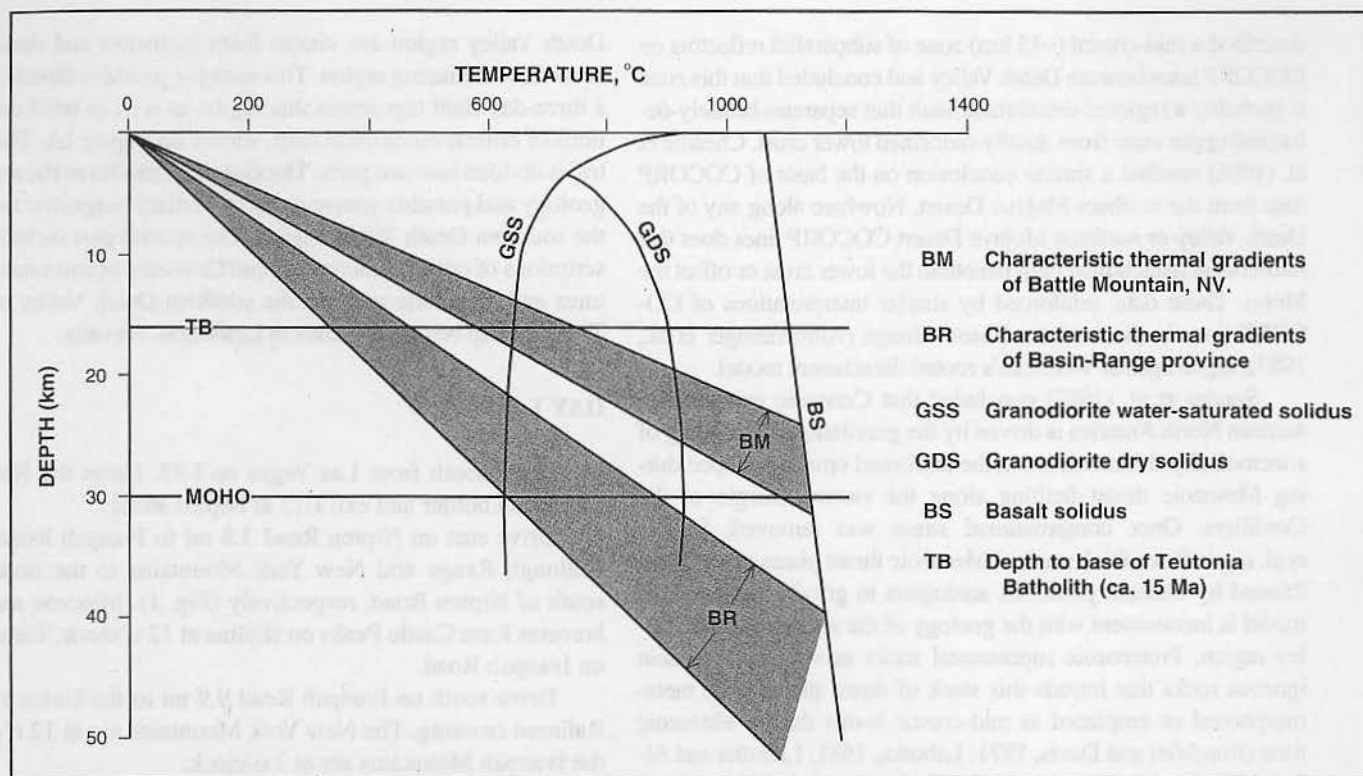
Figure 6. Generalized thermal gradients and solidus curves of igneous rocks in the southern Basin and Range province. Range of thermal gradients characteristic of the Basin-Range region and Battle Mountain from Lachenbruch and Sass (1977). Solidus and liquidus curves from Luth et al. (1964) and Wyllie (1971). Depth to Moho from Serpa et al. (1988); estimated depth to base of Teutonia Batholith (TB) computed from isostatic residual gravity data (Jachens, written commun., 1990) plus postmiddle Miocene uplift of the Kingston Range (Calzia, 1990).

the restite requires higher temperatures to melt. Complete melting does not occur until temperatures approach the basalt dry solidus (BDS).

The tectonic-magmatic model requires that the southern Death Valley region be subjected to extensional stress during late Cenozoic time. Zoback et al. (1981) reported that a uniform back-arc extensional stress field was established by latest Oligocene-early Miocene time throughout the central and southern Basin-Range. The minimum principal stress axis was horizontal and oriented west-southwest–east-northeast as inferred from the trend of Miocene dike swarms, orientation of uniform dip-slip vectors on normal faults, and tilt directions of strata coeval with extension (Zoback et al., 1981).

The minimum principal stress axis was rotated 45° clockwise from west-southwest–east-northeast to west-northwest–east-southeast during middle Miocene time (Zoback et al., 1981). This clockwise rotation was time transgressive and is marked by the initiation of block-style faulting and intrusion of north- to northeast-trending basaltic dikes in the southern Basin-Range 13–10 Ma ago (Eberly and Stanley, 1978), and by east- to northeast-trending range-bounding normal faults and nearly parallel volcanic feeder dikes in the northern Basin-Range ~10 Ma ago (Zoback et al., 1981).

The west-northwest–east-southeast stress orientation has continued to the present day and has produced the Basin-Range

physiography. Basin–Range deformation results from block faulting that penetrates the upper 15 km of the crust and produces north-south and north- to northeast-trending elongate ranges with a range crest to range crest spacing of 25–35 km (Zoback et al., 1981). The ranges are eastward-tilted fault blocks bounded by normal faults; basaltic and bimodal volcanism is associated with this extension (Christiansen and Lipman, 1972).

Wright (1976, 1977) reported that east- to southeast-dipping fault blocks and post 12 Ma normal faults in the southern Death Valley region are compatible with a west-northwest–east-southeast extensional stress field. North- to northwest-trending range-bounding normal faults are influenced by earlier features, such as basement domes in the Black Mountains and the cuspate margins of Mesozoic plutons, and are not reliable indicators of the orientation of the Late Cenozoic regional extensional stress field.

DISCUSSION

Other models of crustal extension in the Great Basin are not consistent with geophysical and geologic data from the southern Death Valley region. Wernicke (1981, 1985) reported that magmatism plays no role relative to the dynamics of crustal extension and concluded that extension is caused by uniform simple shear along a low-angle detachment fault that is "rooted" in the lower crust or the mantle. Serpa et al. (1988)

described a mid-crustal (~15 km) zone of subparallel reflectors on COCORP lines beneath Death Valley and concluded that this zone is probably a regional detachment fault that separates brittlely-deformed upper crust from ductilely-deformed lower crust. Cheadle et al. (1986) reached a similar conclusion on the basis of COCORP data from the northern Mojave Desert. Nowhere along any of the Death Valley or northern Mojave Desert COCORP lines does this mid-crustal detachment fault penetrate the lower crust or offset the Moho. These data, reinforced by similar interpretations of CO-CORP lines in the northern Basin– Range (Allmendinger et al., 1987), argue against Wernicke's rooted detachment model.

Sonder et al. (1987) concluded that Cenozoic extension in western North America is driven by the gravitational unloading of a tectonically-thickened crust; the thickened crust developed during Mesozoic thrust faulting along the eastern margin of the Cordillera. Once compressional stress was removed, Sonder et al. argue that a thick stack of Mesozoic thrust plates would have thinned by tectonic processes analogous to gravity sliding. This model is inconsistent with the geology of the southern Death Valley region. Proterozoic supracrustal rocks as well as Mesozoic igneous rocks that intrude this stack of thrust plates were metamorphosed or emplaced at mid-crustal levels during Mesozoic time (Burchfiel and Davis, 1971; Labotka, 1981; Labotka and Albee, 1988; Beckerman et al., 1982). These supracrustal and igneous rocks are overlain unconformably by 19.1 Ma tuff as well as fanglomerate and lacustrine deposits that predate the inception of extension in the southern Death Valley region (Reynolds, written commun., 1984; Brady, 1985, 1990; Friedmann, 1996). Although evidence of Mesozoic thrust faulting and tectonic thickening of the crust is widespread, regional stratigraphic relations suggest that this thick stack of thrust plates had been eroded, and the subjacent mid-crustal supracrustal and igneous rocks exhumed, prior to late Cenozoic extension in the southern Death Valley region.

CONCLUSION

The close temporal and spatial relation between Late Cenozoic crustal extension and magmatism in the southern Death Valley region suggests a genetic and probably a dynamic relation between these geologic processes. We propose a tectonic-magmatic model consistent with this relation. If the model is correct, then syntectonic, mantle-derived mafic magmas should be cogenetic with coeval, crustally-derived granitic magmas; the granitic magmas should show chemical and isotopic evidence of magmatic interaction with the mafic magmas and should approximate a hydrous minimum or eutectic composition. Test(s) of our model are in progress; some of the results are published (Rämö and Calzia, 1998; Rämö et al., 1999, 2000) or in preparation.

FIELD TRIP ROAD LOG AND DESCRIPTION OF STOPS

Critical outcrops that demonstrate a temporal and spatial relation between crustal extension and magmatism in the southern

Death Valley region are visible from highways and roads that cross this fascinating region. This road log provides directions for a three-day field trip across this region as well as brief descriptions of critical outcrops at stops shown on Figure 1A. The field trip is divided into two parts. The first part introduces the regional geology and possible source rocks of Tertiary magmatic rocks in the southern Death Valley region. The second part includes descriptions of critical outcrops of late Cenozoic extensional structures and magmatic rocks in the southern Death Valley region. The field trip begins and ends in Las Vegas, Nevada.

DAY 1

Drive south from Las Vegas on I-15. Cross the Nevada–California border and exit I-15 at Nipton Road.

Drive east on Nipton Road 3.8 mi to Ivanpah Road. McCullough Range and New York Mountains to the north and south of Nipton Road, respectively (Fig. 1). Miocene andesite breccias form Castle Peaks on skyline at 12 o'clock. Turn south on Ivanpah Road.

Drive south on Ivanpah Road 9.9 mi to the Union Pacific Railroad crossing. The New York Mountains are at 12 o'clock; the Ivanpah Mountains are at 3 o'clock.

Turn east on a dirt road just before and parallel to the Union Pacific Railroad. Drive east on the dirt road 2.0 mi to the third railroad bridge. Turn under the bridge and drive south 1.5 mi on an old pipeline road. Turn left at fork in old pipeline road and continue into Willow Wash.

Stop 1–1. Proterozoic rocks of Willow Wash

A heterogeneous section of supracrustal rocks and orthogneiss are present in Willow Wash. The section of supracrustal rocks is 1.5 km thick and consists of layered mafic rocks and quartzofeldspathic gneiss that are interlayered on a centimeter to meter scale (Elliott, 1986). The mafic rocks form lenticular bodies and consist of plagioclase, hornblende, clinopyroxene, orthopyroxene, and locally biotite. The migmatitic quartzofelspathic gneiss consists of plagioclase, quartz, biotite, garnet, and locally potassium feldspar; sillimanite gneiss and ultramafic rocks are present but rare. The abundance of isoclinal folds and boudinage suggest that the mafic rocks are intensely deformed; metamorphic mineral assemblages suggest that these rocks were derived from a basaltic protolith and were subjected to granulite grade metamorphism. Compositional layering and variation in mineral assemblages suggest that the gneiss was derived from an immature sedimentary protolith such as graywacke. Discordant U-Pb data from 1.98 Ga zircons in the gneiss may be explained by a two stage Pb isotopic evolution model that includes a granulite grade thermal event at 1.71–1.70 Ga (Elliott, 1986).

The orthogneiss consists of biotite augen gneiss. The abundance of intrusive contacts and homogeneous composition suggest that the augen gneiss intrudes the supracrustal rocks and was derived from a biotite granite or granodiorite protolith (Wooden

and Miller, written commun., 1992). Zircons from the augen gneiss yield a U-Pb age of 1.71 Ga (Wooden and Miller, 1990).

Return to I-15 and drive 6.1 mi west (toward Barstow and Los Angeles) to Bailey Road. Exit I-15 at Bailey Road, cross over the freeway, and immediately turn left on a paved road (which becomes a dirt road). Follow this road 0.7 miles east, then 0.45 miles south, to a dilapidated corral. We will walk from here.

Stop 1–2. Ultrapotassic mafic plutonic rocks at Mountain Pass by Gordon B. Haxel, U.S. Geological Survey, Flagstaff, Arizona 86001

Magmatic rocks at Mountain Pass consist of compositionally unique carbonatite pluton that intrudes ultrapotassic silicate rocks. The carbonatite includes bastnäsite ($CeCO_3F$) and parisite ($Ce_2Ca(CO_3)_3F_2$], and is characterized by extreme REE fractionation [$(La/Yb)_{cn}$ = 2000–7000], extraordinary Ba content (14–20 percent BaO; barite phenocrysts are common), and high concentration of F and S (Olson et al., 1954; Watson et al., 1974; Crow, 1984; Castor, 1991; Haxel, in press).

Whereas nearly all other carbonatites are associated with sodic (nephelinitic) silicate igneous rocks, the Mountain Pass carbonatites is associated with ultrapotassic phlogopite-rich shonkinite (melanosyenite). The ultrapotassic shonkinite (K_2O/Na_2O = 4–8 percent) is remarkable for elevated abundances of many incompatible elements, including K (= 8 percent K_2O), Ba (= 7000 $\mu g/g$), Rb (400), Cs (8), Th (80–300), and LREE (La 400, Ce 800). Whole-rock fluorine concentrations, 0.9–1.4 percent, are among the largest known in unaltered silicate igneous rocks. The most primitive shonkinite dikes of the Mountain Pass district have compositions (mg = 0.76, Cr ≈ 500, Ni ≈ 300 $\mu g/g$) indicating that they are primary, mantle-derived magmas. Their very small volume, high volatile content, and high incompatible element abundances further argue against appreciable crustal assimilation. The primitive shonkinites have elevated Th/U (≈ 9), characteristic of the Mojave lithospheric province. Some primitive shonkinite dikes are synplutonic and probably parental with respect to several small shonkitite-syenite stocks. Apatite from the shonkinite yields a U-Pb age of 1.41 Ga (DeWitt et al., 1987).

At this stop we will examine excellent exposures of synplutonic shonkinite dikes within a shonkinite-syenite stock. The synplutonic dikes display an intriguing variety of shapes, patterns, and textures, collectively indicating that shonkinite magma was intruded repeatedly during solidification of the syenite stock, and that shonkinite mingled and locally mixed with syenite. Early dikes were extensively back-intruded and disrupted by their syenite host, so that they now form trains of ovoid to amoeboid shonkitite inclusions within the syenite. Later dikes partially maintain their original tabular shapes and locally have fine-grained margins against the host syenite. But, even these younger dikes were locally intruded or veined by syenite or leucosyenite. Most of the shonkinite inclusions and dikes have associated with them irregular, dense to diffuse

masses or patches of pegmatoid syenite (some amphibole-rich), gradational outward into normal syenite. Presence of this pegmatoid syenite probably reflects nucleation of crystals and/or concentration of volatiles adjacent to the shonkinite bodies. The youngest shonkinite dikes both are crosscut by and crosscut syenoaplite dikes. One outcrop clearly shows that late shonkinitic and aplitic magmas coexisted (apparently with minimal mingling) and moved through the syenite stock along the same channel. *These informative and important shonkinite-syenite relations are not well exposed anywhere else in the Mountain Pass district.* **Please do not use your hammer and destroy the evidence!** *Samples of shonkinite and syenite are readily available nearby from near-source float.* Time permitting, we will walk or drive to the top of a nearby hill for a brief overview of the Mountain Pass REE deposit.

Return to I-15 and drive south 9.0 mi to Cima Road; the Clark and Ivanpah Mountains are on the north and south sides, respectively, of the freeway. These mountains open into Shadow Valley about 6 miles south of Bailey Road. Cima Dome and Teutonia Peak are at 8 o'clock, the Pliocene and Holocene Cima volcanic field at 11 o'clock, and the Halloran Hills are at 1 o'clock. The Kingston Range forms the skyline at 3 o'clock.

Exit I-15 at Cima Road. Cross over the freeway and drive south 7.6 mi to unnamed dirt road just north of old corral on east side of Cima Road.

Turn east onto dirt road and drive 4.6 mi toward the Ivanpah Mountains on the skyline. Dirt road forks within 100 yds of Cima Road; take the south fork and enter a very healthy Joshua Tree forest.

Stop 1–3. Jurassic Ivanpah granite

Cordilleran plutons related to Mesozoic subduction are well exposed in the southern Death Valley region. The petrography and geochemistry of these Mesozoic rocks were studied in detail by Beckerman et al. (1982). They recognized a minimum of six noncomagmatic granitoid suites that together comprised the ~3000 km² Cretaceous–Jurassic Teutonia Batholith. Current usage, however, defines the Teutonia Batholith to include only the Cretaceous plutons (U.S. Geological Survey, 1991). We have recently completed a detailed geochemical and Nd-Sr-Pb isotopic study on critical samples of the Mesozoic (Middle Jurassic–Late Cretaceous) plutons of the southern Death Valley region (Rämö et al., 2000). The descriptions of the Mesozoic plutons are mainly based on Beckerman et al. (1982) and our own observations; we will briefly refer to our new isotopic data in order to speculate on the petrogenesis and magmatic evolution of the Mesozoic plutons.

The 145 Ma (U.S. Geological Survey, 1991) Ivanpah granite is a light tan and coarse grained syenogranite that shows a faint magmatic foliation. It is intruded by the Cretaceous Teutonia adamellite that underlies most of Cima Dome. The Ivanpah granite ranges from seriate to coarse porphyritic in texture and has a high proportion of alkali feldspar to plagioclase

(Beckerman et al., 1982). The main silicates comprise alkali feldspar, quartz, plagioclase, and biotite. Minor amounts of hornblende, apatite, titanite, allanite, zircon, fluorite, and rutile as well as secondary muscovite are present. Geochemically, the Ivanpah granite is metaluminous to marginally peraluminous and it shows evidence for thorough autometasomatic modification that has resulted, for instance, in an extremely high Rb/Sr and a flat chondrite-normalized REE pattern with a very deep Eu anomaly. The Rb-Sr isotopic system of the rock has been severely disturbed, but the Nd isotopic composition (ε_{Nd} of –13.4) indicates a high proportion of cratonic material in the protolith.

Return to vehicles and Cima Road. Turn south, and drive 3.1 mi to Valley View Ranch Road.

Turn west on Valley View Ranch Road and drive 1.8 mi to the white ranch house. Turn left on the dirt road just before the ranch house and drive toward the water tanks and windmill. Go past the corral on left and park in the wide area. Watch where you step for reasons that will become obvious upon your arrival!

Stop 1–4. Cretaceous Teutonia adamellite and the Teutonia Batholith

Cretaceous plutonic rocks of the southern Death Valley region are most abundant in the ~3000 km² Teutonia Batholith beneath Cima Dome. Cretaceous granitoids also are present in the Owlshead Mountains; these rocks, however, may represent allochthnohous blocks of the Teutonia Batholith disrupted by Tertiary extension (Brady, 1985). Our new isotopic data suggest that the allochthonous blocks of Teutonia are distinct from the autochthonous rocks at Cima Dome. The former have, on average, lower ε_{Nd}, higher Sr_i, and more radiogenic uranogenic Pb isotopic ratios and thus show a more cratonic character (Rämö et al., 2000).

The 97 Ma (DeWitt et al., 1984) Teutonia adamellite is the typical granitoid type of the Teutonia Batholith at Cima Dome. It is a light tan, medium- to coarse-grained massive syenogranite that occasionally grades into coarse quartz alkali feldspar syenite. It intrudes cratonic rocks and the Jurassic Ivanpah granite (Stop 1–3) and is quite leucocratic with only minor amounts of biotite, secondary muscovite, apatite, allanite, zircon, and ilmenite. Like the Ivanpah granite, the Teutonia adamellite is metaluminous to marginally peraluminous. The initial Nd (ε_{Nd} of –13.5) and Sr (Sr_i of 0.7170) isotopic composition of the adamellite suggests that it represents a mixture of mantle and Proterozoic crust (Rämö et al., 2000).

Return to Cima Road, turn south, and drive 8.1 mi to Cima. Kessler Peak and Teutonia Peak on east and west sides, respectively, of Cima Road. Outcrops of the Cretaceous Kessler Spring adamellite are present on both sides of the road at the crest of Cima Dome. Ivanpah Valley is in the foreground once over the crest of the dome. Mountain ranges south of Ivanpah Valley include the New York Mountains at 9:30 o'clock, Providence Mountains on distant skyline at 1 o'clock, and Mid Hills at 12 o'clock. Note: Cima Road becomes Cima–Kelso Road at Union Pacific Railroad crossing. Cross the railroad and continue on Cima–Kelso Road to Cima. OTR loves to call his wife and family in Helsinki, FI from the phone booth at Cima!

Continue south and west 4.6 mi from Cima to Cedar Canyon Road. Small gray hills on both sides of Cima–Kelso Road consist of Proterozoic cratonic rocks of uncertain protolith.

Turn south on Cedar Canyon Road, immediately cross the railroad tracks, and drive 6.4 mi to Black Canyon Road. Proterozoic cratonic rocks intruded by the Cretaceous Mid Hills adamellite forms the skyline at 12 o'clock.

Continue past Black Canyon Road 5.0 mi to Rock House Spring. Cedar Canyon Road forks to right once you exit the canyon cut in Tertiary volcanic rocks. Stay on the main road and turn south into dirt driveway toward the rock house on the skyline. Turn south along the fence line and park in the wash. CAREFUL, it's sandy. May need 4-wheel drive to get out of the wash.

Stop 1–5. Cretaceous Rock Spring monzodiorite

The 97 Ma (U.S. Geological Survey, 1991) Rock Spring monzodiorite is the most mafic granitoid rock of the Teutonia Batholith. Covering much of the Mid Hills, it occurs as a compositionally zoned pluton with biotite-clinopyroxene diorite along the northern edge and hornblende-biotite quartz monzodiorite and granodiorite to the south (Beckerman et al., 1982). The rock is dark gray to brown in color, medium- to coarse-grained, equigranular, and characteristically includes fine-grained mafic autoliths. Besides plagioclase (occasionally present as microphenocrysts), alkali feldspar, and quartz, the rock includes biotite, hornblende, occasional clinopyroxene, apatite, titanite, zircon, oxide, and epidote. Geochemically, the Rock Springs monzodiorite is clearly more mafic than the Jurassic Ivanpah granite (Stop 1–3) and the Cretaceous Teutonia Peak adamellite (Stop 1–4). It is metaluminous, low in SiO_2 (55wt%–65 wt%) and has distinctly more radiogenic initial Nd (ε_{Nd} of –6.6) and less radiogenic initial Sr (Sr_i of 0.7074) isotopic composition. Accordingly, the protolith of the Rock Springs monzodiorite probably had a less cratonic character than that of the Ivanpah granite and Teutonia adamellite.

Return to Cedar Canyon Road, turn west, and drive 5.0 mi to Black Canyon Road. Tertiary volcanic rocks are at 12 o'clock.

Turn south on Black Canyon Road and drive south 4.1 mi through Round Valley and into Black Canyon. Large outcrops of Mid Hills adamellite are on west side of Black Canyon Road near intersection with road into Mid Hills Campground. Park in wide spot on east side of Black Canyon Road in Black Canyon.

Stop 1–6. Cretaceous Black Canyon gabbro

The Black Canyon gabbro is one of the few exposed Mesozoic mafic plutonic rocks in the southern Death Valley region. It forms an equant stock, ~1 km², that intrudes the 93 Ma (U.S. Geological Survey, 1991) Mid Hills adamellite (Beckerman et al., 1982). The gabbro is very heterogeneous with alternating hornblende and plagioclase-rich zones and mafic enclaves. The main mineral phases are plagioclase and hornblende; accessory

minerals comprise clinopyroxene, biotite, apatite, titanite, and oxides. Geochemically the Black Canyon gabbro is tholeiitic and shows a wide range of fractionation. The initial Nd and Sr isotopic composition of the gabbro is quite juvenile (ε_{Nd} of–3.2; Sr_i of 0.7060), which suggests that the gabbro may have initially been derived from a slightly depleted asthenospheric source (Rämö et al., 2000).

CAREFULLY turn around and return to Cedar Canyon Road. Turn west on Cedar Canyon Road to Cima–Kelso Road.

Turn south on Cima–Kelso Road and drive 18.0 mi to Kelso. Old Dad and Kelso Mountains form skyline at 10–12 o'clock; Cima Dome and Teutonia Peak are at 2 o'clock. Low gray hills at base of Cima Dome are cratonic rocks; dark bumps at crest of Cima Dome are cinder cones in Cima volcanic field. Winding dirt road at 12 o'clock is the Mojave Road. This road was an Indian trail, military road, and the major highway between Los Angeles and the Colorado River until 1883 when it was replaced by the railroad. As we approach Kelso, the Kelso Dunes are visible in the middle foreground. The Granite Mountains form the skyline behind and to the south of the dunes.

Turn north on the Kelbaker Road at the stop sign in Kelso and drive 36.3 mi to Baker. Kelso was founded in 1905 as a water stop on the railroad; the depot was built by the Union Pacific Railroad in 1924. The Kelso Depot served as a roadhouse for railroad employees as well as a telegraph office, waiting room, and restaurant until it was closed in 1985; it is one of two Spanish style depots still in existence along the railroad. Approximately 2000 people lived in Kelso during World War II to mine iron ore in the Providence Mountains.

The Kelso Mountains form the skyline at 12 o'clock immediately after leaving Kelso. Approximately 12.3 mi north of Kelso, the Kelbaker Road crosses the crest of the Kelso Mountains; Old Dad Mountains form the skyline at 11 o'clock and cinder cones in the Cima volcanic field are visible at 12 o'clock. Approximately 10.5 mi north of the crest of the Kelso Mountains, a 0.6 Ma basalt flow unconformably overlies ca. 2.0 Ga cratonic rocks on the east side of Kelbaker Road. This is truely a great unconformity where ~2 b.y. of Earth's history is lost across this contact!

Approximately 13.0 mi from the crest of the Kelso Mountains, the Kelbaker Road makes a hard left turn and points directly at Baker at the base of the Soda Mountains. Soda dry lake is visible between 11 and 1 o'clock, the Halloran Hills are at 2 o'clock, and the Avawatz Mountains form the skyline between the Soda Mountains and Halloran Hills.

Cross I-15 and the Kelbaker Road becomes Highway 127.

Enter Baker and turn west onto Baker Blvd at the stop sign. Drive 0.3 mi west, cross the Mojave River, and stop at the Royal Hawaiian Motel on the north side of Baker Blvd. End of first day.

DAY 2

From Royal Hawaiian Motel, turn east on Baker Blvd and drive 0.3 mi to stop sign at Highway 127.

Turn north on Highway 127, drive 20.3 mi to the dirt road to Old Mormon Spring. As you leave Baker, Baker Airport is on the west side of the highway; the Soda Mountains form the skyline behind the airport. The Avawatz Mountains are at 11 o'clock and the Halloran Hills are on the skyline at 1 o'clock. Approximately 10.2 mi north of Baker, cross a drainage divide into Silurian Valley. Here, the Avawatz Mountains are at 10 o'clock, the Silurian Hills are at 1 o'clock, and the west end of the Halloran Hills are at 3 o'clock.

Turn west on dirt road that is parallel to diversion ditch and drive 8.3 mi west to Old Mormon Spring at base of Avawatz Mountains. The dirt road is very difficult to find. If you get lost, dirt road is 0.15 mi north of Emergency Call Box 127–192 on Highway 127.

Stop 2–1. Jurassic granodiorite of the Avawatz Mountains and the Mule Spring thrust

The 177 Ma (DeWitt et al., 1984) granodiorite of the Avawatz Mountains serves as an example of the relatively few Jurassic plutonic rocks of the southern Death Valley region. It is a mafic, medium-grained granodiorite with biotite and hornblende as the main mafic silicates. Biotite and hornblende are found as poikilitic grains enclosing auhedral epidote and titanite crystals. Other accessory minerals include zircon, apatite, and oxide. The granodiorite is metaluminous (A/CNK = 0.87) and relatively low in SiO_2 (64 wt%). Its initial Nd (−8.1) and initial Sr (0.7083) isotopic composition suggest that the granodiorite represents a mixture of lithospheric mantle and Precambrian crust (Rämö et al., 2000).

The Mule Spring thrust fault trends east-west then curves to the southeast along the north and east side of the Avawatz Mountains, respectively; it dips steeply to the south along the northern side of the mountains and 29°–33°W at Old Mormon Spring (Troxel and Butler, 1998). The Mule Spring fault cuts out the Garlock fault as well as the west and central branches of the southern Death Valley fault zone along the northern side of the Avawatz Mountains. The eastern branch of the southern Death Valley fault zone is deformed and parallels the Mule Spring fault around the east side of the mountains. Quaternary gravels are tectonically overlain by the Jurassic granodiorite of the Avawatz Mountains along the Mule Spring fault at Old Mormon Spring (Fig. 7). These tectonic relations suggest that the Mule Spring fault is younger than late Cenozoic extensional structures in the southern Death Valley region, and that the regional stress field has changed from extension to compression along the southern boundary of this region.

Return to Highway 127, turn north, and drive 11.0 mi to Harry Wade Exit route. While driving north on Highway 127, note the fault scarp of the eastern branch of the southern Death Valley fault zone in the alluvial fans at the base of the Avawatz Mountains at 9 o'clock. The southern Salt Spring Hills are at 11 o'clock, Saddlepeak Hills form skyline between 11 and 12 o'clock, Sperry Hills and Alexander Hills form low ridge in
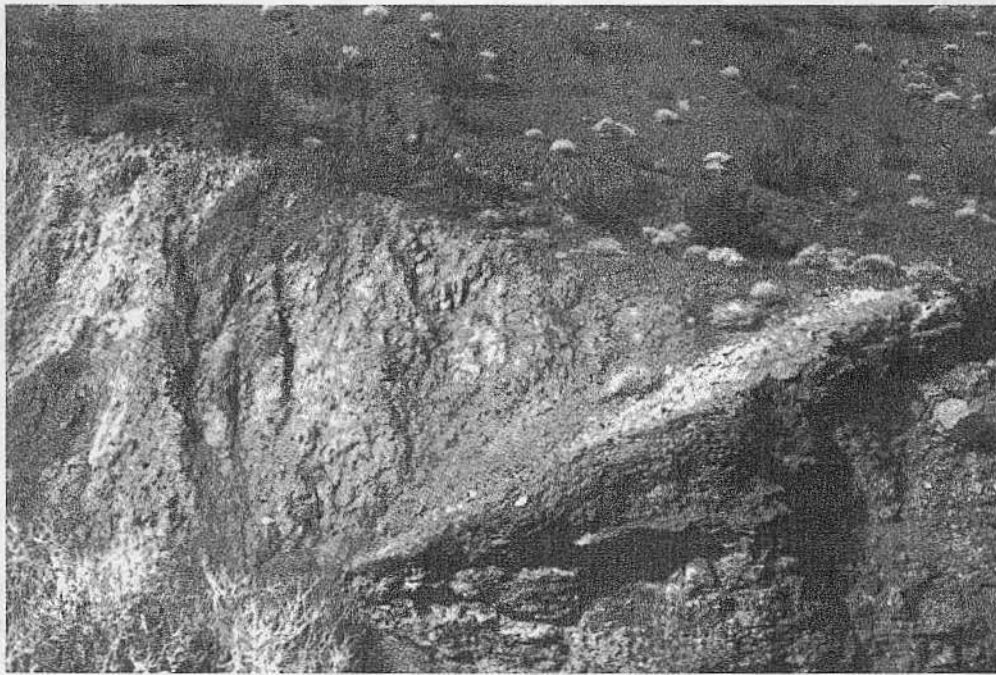
Figure 7. Jurassic granodiorite of the Avawatz Mountains thrust over Quaternary gravels at Old Mormon Spring, eastern Avawatz Mountains.

middle distance, Dumont Dunes at 12 o'clock, Valjean Hills and Valjean Valley at 1 o'clock, and Silurian Hills at 3 o'clock. Kingston Range forms skyline behind the Valjean Hills.

Approximately 8.8 mi north of the Old Mormon Spring Road, Highway 127 crosses Holocene Lake Dumont lacustrine deposits. Notice the landslide breccia of carbonate rocks at the southeast end of the Salt Spring Hills at 3 o'clock. The landslide breccia consists of the Bonanza King Formation, Sultan Limestone, and the Bird Spring Formation tectonically overlying 12.8 Ma basaltic andesite. See text for tectonic significance of this and other carbonate breccias in Valjean Valley.

Turn west on Harry Wade Exit Road, drive 6.2 mi, and stop across the road from the sign to Saratoga Springs. Once on Harry Wade Exit Road, the Avawatz Mountains are at 9 o'clock, the Owlshead Mountains are on the skyline at 12 o'clock, and the Saddlepeak Hills are at 3 o'clock. The Panamint Range is on skyline behind the Saddlepeak Hills. Low calico colored hills that eventually become visible at 11 o'clock are the Noble Hills. The Black Mountains form the skyline behind Saratoga Springs and the Saratoga Hills on the north side of the road.

Stop 2–2. Southern Death Valley fault zone

The southern Death Valley fault zone trends north-south and is divided into three branches that cut Tertiary fanglomerate deposits in the Noble Hills (Troxel and Butler, 1998). Each branch has a component of right-lateral slip and records a secular migration of displacement; the youngest movement is recorded at the northern and easternmost end of each branch. As

the fault branches extend southeastward, they are cut out or merge with the Mule Spring fault (Troxel and Butler, 1998).

The oldest fanglomerate deposit, here named the western fan, tectonically overlies pre-Tertiary crystalline rocks in the Avawatz Mountains and is ~300 m thick. The western fan consists of conglomerate and siltstone; cross bedding and graded beds are common. The conglomerate consists of boulders of diorite, quartz monzonite, carbonate rocks, andesite, and ptygmatic-folded gneiss; all of these rocks were derived from the Avawatz Mountains (Troxel and Butler, 1998). The western fan is tectonically overlain by the central fanglomerate deposits.

The central fanglomerate deposit dips steeply to the south and is also ~300 m thick. This fan consists of fine-grained sandstone, thin bedded siltstone, and gypsum; local beds of limestone and sheets of megabreccias are common. The gypsum beds are highly contorted or attenuated and often resemble toothpaste; the megabreccias consist of quartz monzonite or gneiss with minor andesite. The central fanglomerate deposit is tectonically overlain by the eastern fanglomerate deposit.

The eastern fanglomerate deposit, or eastern fan, consists of a basal conglomerate overlain by siltstone; salt and silty salt beds; gypsum; and siltstone with celestite, chert, and limestone. This fan is complexly folded so its thickness is unknown.

The composition of the fanglomerate deposits helps constrain displacement on the southern Death Valley fault zone. The combination of quartz monzonite, gneiss, and andesite megabreccias in the central fanglomerate deposit could only be derived from a point source in the northeastern Owlshead Mountains; andesite from this area yield a whole-rock age of

10.6 Ma (Butler, 1984). If Butler's correlation is correct, then the southern Death Valley fault zone has up to 35 km of right-lateral displacement in the last 11 m.y.

Return to the vehicles and drive 14.3 mi north on Harry Wade Exit Road to the Amargosa River.

Enter Death Valley National Park approximately 1.4 mi north of Stop 2–1. The road crosses the east strand of the southern Death Valley fault zone approximately 5.1 mi north of the park boundary. The low gravel-covered hill on the east side of the road is the east fan cut by the southern Death Valley fault zone.

The road into the Owlshead Mountains intersects the Harry Wade Exit Road ~6.5 mi north of the park boundary. Continue north on the Harry Wade Exit Road; DO NOT turn left to the Owlshead Mountains. Small peak in foreground at 10 o'clock is the western fan cut by the southern Death Valley fault zone. The Owlshead Mountains form skyline behind this low peak. Also at this intersection, Death Valley is visible at 12 o'clock and the Black Mountains are at 2 o'clock.

Cross the Amargosa River, drive ~0.5 mi north and stop alongside road.

Stop 2–3. Owlshead Mountains and the Teutonia Batholith

The Owlshead Mountains consist of 95 Ma quartz monzonite and granite that are petrographically similar to the 97 Ma Teutonia adamellite in the Teutonia Batholith (Calzia, 1974). Isostatic gravity data suggest, however, that magmatic rocks in the Owlshead Mountains are <5 km thick (Blakely, personal commun., 2000); the Teutonia Batholith is >12 km thick (Calzia, 1990). This variation in thickness may be caused by tectonic thinning of an allochthonous block of the Teutonia Batholith during an intense period of crustal extension (Brady, 1985), or in situ thinning of a pluton that resembles the Teutonia adamellite. Our recent isotopic data suggest that magmatic rocks in the Owlshead Mountains are distinct from the Teutonia adamellite (Rämö et al., 2000); gravity and magnetic data suggest that the Owlshead Mountains were extended ~60% (Jachens and Calzia, 1998). Combined, these data suggest that quartz monzonite and granite in the Owlshead Mountains do not correlate with the Teutonia adamellite and the Owlshead Mountains are autochthonous.

Return to the vehicles and drive north on Harry Wade Exit Road 12.6 mi to intersection with Highway 178. Gold color hill at 11 o'clock is the south end of the Confidence Hills. Dark outcrops in the Owlshead Mountains on the skyline behind the Confidence Hills consist of gneiss, Crystal Spring Formation, and diabase. The Panamint Range forms the distant skyline at 12 o'clock.

Turn east on Highway 178 toward Shoshone and stop on south side of road. Dark hill at the north end of Confidence Hills is Shoreline Butte. Shoreline Butte consists of 1.7 Ma basalt cut by numerous strand lines of Pleistocene Lake Manly. Low hill west of Highway 178 consists of alluvial fan deposits at Ashford Mill. Small reddish hill in floor of Death Valley between Shoreline Butte and alluvial fans at Ashford Mill is a 0.7 Ma cinder

cone offset 0.3 km by the southern Death Valley fault zone. Red and rusty colored hills at 1 o'clock consist of landslide breccias from the Black Mountains.

Stop 2–4. Amargosa chaos

Noble (1941) reported that the southern Black Mountains consist of complexly folded and faulted rocks that he divided into three lithologic-structural units. The oldest unit consists of autochthonous gneiss intruded by Proterozoic, Mesozoic, and Tertiary diabase and granitic rocks. The autochthonous gneiss is tectonically overlain by an allochthonous plate composed largely of nested fault blocks of Proterozoic, Paleozoic, and Tertiary sedimentary, volcanic, and granitic rocks. These allochthonous rocks are overlain by autochthonous cover rocks consisting of Cenozoic fanglomerate, basalt, and alluvium. Noble (1941) named the tectonic boundary between the gneiss and allochthonous rocks the Amargosa thrust; he named the fault blocks within the allochthonous plate the Amargosa chaos. The Amargosa thrust was renamed the Amargosa fault by Wright et al. (1991).

Noble (1941) divided the Amargosa chaos into the Virgin Spring, Calico, and Jubilee phases. The Virgin Spring phase is structurally the lowest phase and is locally overlain by the Calico or Jubilee phase; the relative ages of the Calico and Jubilee phases is uncertain because they are never in contact with each other. Each phase is cut by innumerable normal and strike-slip faults. The normal faults flatten at depth; some merge with the Amargosa fault, others cut the Amargosa fault and the autochthonous gneiss (Wright and Troxel, 1984).

The Virgin Spring phase consist of a chaotic mosaic of tightly packed blocks of allochthonous gneiss, Pahrump Group, and miogeoclinal rocks; locally, gneiss is depositionally overlain by Proterozoic rocks within individual blocks. Each block is elongated and bounded by faults and resembles whales or large tadpoles in cross section. Bedding within the sedimentary rocks is minutely fractured yet is clearly discernable and sharply truncated at the boundary of each block. The Virgin Spring phase is ~610 m thick but its original thickness is unknown; it is tectonically overlain by the Calico phase of the Amargosa chaos or is unconformably overlain by the Funeral Formation (Noble, 1941).

The Calico phase of the Amargosa chaos is ~300 m thick and consists of the Shoshone Volcanics. The Calico phase is intimately broken by faulting but is not as chaotic as the Virgin Spring phase (Noble, 1941; Wright and Troxel, 1984).

The Jubilee phase consists of Tertiary fanglomerate deposits, sedimentary rocks, and tuff intimately associated with megabreccia sheets of miogeoclinal rocks and Miocene granitic rocks. The Jubilee phase is ~300 m thick but this too is a minimum thickness because the Jubilee phase is unconformably overlain by the Funeral Formation (Noble, 1941; Wright and Troxel, 1984).

Wright et al. (1991) reported that the Amargosa fault is intruded by 6.4–8.7 Ma silicic cupolas, stocks, and plutons, and locally is depositionally overlain by 7.5–8.5 Ma Shoshone

Volcanics in the southern Death Valley volcanic field. Similar geometry and chronology of faults in the Resting Spring Range to those in the southern Black Mountains led Wright et al. to conclude that 11.7–9.3 Ma eastward tilting of the Resting Spring Range was synchronous with movement on Amargosa fault and development of Virgin Spring phase of the Amargosa chaos. These regional observations suggest that the Amargosa fault and Amargosa chaos are older than 6.4 Ma and younger than 11.7 Ma.

Wright and Troxel (1984) concluded that the Amargosa chaos is an extensional feature that formed in situ on the underside of rotated fault blocks or in the vicinity of detachment faults where normal faults flatten and join at shallow depths. Topping (1993) concluded that granite megabreccias in the Jubilee phase were derived from rock avalanche deposits in the Sperry Hills; his rock avalanche deposits were derived from the granite of Kingston Peak in the Kingston Range and were faulted to their present position by the right-lateral Grand View fault. We agree with Topping in that his rock avalanche deposits in the Sperry Hills (our landslide breccias of the granite of Ibex Pass) are allochthonous blocks of the granite of Kingston Peak. We find, however, no geophysical or geologic evidence of the Grand View fault south of Highway 178 or east of the Sperry Hills. The fault along the southwest side of the Alexander Hills and Kingston Range is a west-dipping normal fault with hundreds to thousands of meters of stratigraphic throw.

Return to the vehicles and drive 7.6 mi east on Highway 178 through the Amargosa chaos in the Black Mountains. Note 4.0–4.8 Ma basalt interbedded with the Funeral Formation north of the highway ~0.5 mi east of Jubilee Pass. Stop and park along the north side of Highway 178 ~2.7 mi east of Jubilee Pass.

Stop 2–5. Extensional faulting in the Amargosa chaos

An excellent example of faulting in the Virgin Spring phase of the Amargosa chaos is exposed on the north slope of a small hill on the south side of Highway 178. This hill is ~60 m high and is locally known as Exclamation Point because of comments made by geologists upon recognition of the rocks in this hill. These rocks include the Middle Proterozoic Crystal Spring Formation tectonically overlain by the Late Proterozoic Noonday Dolomite. At its type locality in the Kingston Range, the lower member of the Crystal Spring Formation unconformably overlies gneiss and consists of a basal conglomerate overlain by 410 m of arkosic and feldspathic sandstone and purple mudstone. The lower member is conformably overlain by 160 m of stromatolitic limestone and dolomite with a chert cap rock. The middle carbonate member is conformably overlain by 775 m of sandstone and siltstone interbedded with five dolomite marker beds. All of these rocks are intruded by diabase sills that are 330 m thick and unconformably overlain by the Noonday Dolomite (Calzia, 1990). Save for the upper member, all of these rocks are present at Exclamation Point. The gray and red-stained rocks at the base of the hill are sheared gneiss. Fault bounded lenses of arkosic sandstone and siltstone are tectonically over-

lain by dark green lenses of diabase. The diabase is tectonically overlain by reddish brown lenses of limestone and dolomite, which, in turn, are tectonically overlain by yellow gray Noonday Dolomite. Assuming an original thickness similar to that in the Kingston Range, extensional faulting in the Virgin Spring phase tectonically attenuated the Crystal Spring Formation and diabase sills at Exclamation Point by 93%, yet the original stratigraphy is preserved and recognizable.

Continue east on Highway 178 to Salsberry Pass. Calico colored hills in middle distance on the north side of the highway consist of 7.5–8.5 Shoshone Volcanics; dark flow that overlies the Shoshone Volcanics is the 7.5 Ma basalt of Epaulet Peak. As you drive east, notice that the Shoshone Volcanics get thicker and thicker.

Continuing east, the Shoshone Volcanics form the skyline at 10 o'clock, Sheephead Peak (consisting of pre-Shoshone Volcanics) is the highest peak at 11 o'clock, Sheephead Pass is at 12 o'clock, and the Black Mountains form the skyline at 1 o'clock. The first peak north of Sheephead Pass consists of 10.4 Ma dacite.

Drive 1.2 mi east of Salsberry Pass; stop and park along the south side of Highway 178. Looking north, the Shoshone Volcanics are overlain by Greenwater Volcanics at 9 o'clock, the granite of Miller Springs forms the skyline in the middle distance at 11 o'clock, the 9.8 Ma Shoshone pluton (the World's youngest rapakivi granite) is at 12 o'clock, and pre-Shoshone Volcanics are at 3 o'clock. Dark outcrops of Greenwater Volcanics are present in the floor of Greenwater Valley and at the crest of the Shoshone pluton. Also note that the Shoshone pluton deforms its volcanic cover around the southern margin of the pluton.

Stop 2–6. Southern Death Valley volcanic field

Plutonic and volcanic rocks in the southern Death Valley volcanic field are described in the text and by Wright et al. (1991); it would be redundant to repeat those descriptions here. The reader is referred to the above sources for a description of this magmatic province; we will point out the salient features listed above.

Return to the vehicles and drive 10.0 mi east on Highway 178 to intersection with Highway 127. The Greenwater Valley Road crosses Highway 178 approximately 2.8 mi east of the last stop. At this intersection, the Shoshone and Greenwater Volcanics are at 9–10 o'clock, the Shoshone Volcanics are at 12–1 o'clock, the Resting Spring and Nopah Ranges are in the middle distance, and Charleston Peak in the Spring Mountains, NV form the distant skyline at 11 o'clock.

Turn south on Highway 127, drive 1.6 mi to the Shoshone Inn on the west side of the highway in Shoshone. End of second day.

DAY 3

From Shoshone Inn, turn south on Highway 127 5.7 mi to the intersection with the road to Tecopa. The highway cuts

through the Pliocene and Pleistocene Tecopa lake beds. The Resting Spring Range is at 9 o'clock, Tecopa Peak at 12 o'clock, and Dublin Hills at 3 o'clock. The Avawatz Mountains form the skyline behind Tecopa Peak.

Turn east at intersection and drive 2.7 mi to stop sign in Tecopa. The road crosses the Tecopa lake beds; the Kingston Range forms the skyline at 11 o'clock. The World famous Tecopa Hot Springs (OTR's favorite desert spa—it's the closest spa we have to an original Finnish sauna in the southern Death Valley region!) is just to the left of the stop sign in Tecopa.

Continue on the road and cross over a hill of Late Proterozoic Stirling Quartzite and take the east fork in the road to a stop sign at the intersection with the Old Spanish Trail Highway.

Turn east at the intersection and drive 1.6 mi on the Old Spanish Trail Highway to the intersection with the Furnace Creek Road.

Turn south on the Furnace Creek Road and drive 12.6 mi to Smith Talc Road. The Furnace Creek Road immediately curves to the east after the intersection; the Nopah Range is at 12 o'clock after the curve. Dark rocks at the south end of the Nopah Range are cratonic rocks; lighter rocks to the north are Proterozoic miogeoclinal rocks.

The abandoned town site of Noonday is ~7.0 mi from the intersection of the Furnace Creek Road with the Old Spanish Trail Highway. Numerous tailing piles from Pb-Zn-Ag mines at the base of the Proterozoic Noonday Dolomite are visible at 9 o'clock.

The Furnace Creek Road ends at the Smith Talc Road. Follow the pavement to the south and east into the Kingston Range. The dirt road heading north at the end of the Furnace Creek Road is the Mesquite Valley Road. We will return to Las Vegas on the Mesquite Valley Road.

Drive 6.1 mi east on the Smith Talc Road to the Crystal Spring mine. The Kingston Range and Beck Canyon are at 12 o'clock. The 12.4 Ma granite of Kingston Peak is south of Beck Canyon; the Middle Proterozoic Pahrump Group is north of Beck Canyon. Rusty outcrops low on the north side of Beck Canyon consist of the Crystal Spring Formation; the white patches are talc. The talc formed by contact metamorphism of dolomite in the Crystal Spring Formation during intrusion of 1.08 Ga diabase sills. The gray cliffs above the Crystal Spring Formation consist of the Beck Spring Dolomite; the reddish outcrops in the upper half of the canyon wall consist of the Kingston Peak Formation. The tan cliff-former at the top of the hill is the Noonday Dolomite. The stratigraphy at this end of Beck Canyon is complicated by numerous listric normal faults that trend north-south along the west side of the Kingston Range.

The Crystal Spring mine is the first large talc mine on the north side of the road in the Kingston Range. Here, the Crystal Spring fault displaces the Crystal Spring Formation and talc ~1.4 km to the southwest; the displaced block of talc and tailing piles at the Omega mine are visible south of the road. The Crystal Spring fault also cuts the Kingston Range detachment fault

on the road into the Crystal Spring mine. Dark rocks on the east side of the mine road are gneiss.

Drive 0.6 mi east of the Crystal Spring mine. Stop and park opposite a wide sandy wash on the north side of the road.

Stop 3–1. The Kingston Range detachment fault

The Kingston Range detachment fault is part of the eastern breakaway zone of the Death Valley extended terrain. It dips as much as 15°SW and separates highly extended Proterozoic, Paleozoic, and Tertiary sedimentary rocks as well as 12.5 Ma syntectonic volcanic rocks in the upper plate from relatively unfaulted Proterozoic gneiss in the lower plate. The Kingston Range detachment fault cuts 16.0 Ma (Friedmann, 1996) ash and is cut (Wright, 1968) and deformed (Calzia et al., 1987) by the granite of Kingston Peak. Reconstruction of contacts within the miogeoclinal section suggests that cumulative horizontal displacement of the upper plate is ~6 km to the southwest.

Return to the vehicles and continue east toward the top of Beck Canyon. Turn north at the fork to bypass the Beck iron mine. Drive out of Beck Canyon and continue east past ranch house(s) at Horse Thief Springs. Stop and park on the south side of the road 0.8 mi east of Horse Thief Springs.

Stop 3–2. The granite of Kingston Peak

The granite of Kingston Peak forms an elliptical batholith, 14.6 km long and 10.5 km wide, in the center of the Kingston Range. The granite is divided into feldspar porphyry, quartz porphyry, and aplite facies based on textural variations and intrusive relations. The feldspar porphyry and quartz porphyry facies are characterized by rapakivi textures and miarolitic cavities and contain mafic xenoliths petrographically and chemically similar to volcanic rocks in the Resting Springs Formation; the aplite facies intrudes and is locally gradational into the feldspar porphyry and quartz porphyry facies. Biotite and hornblende from the feldspar porphyry facies yield concordant K-Ar ages of 12.1 and 12.4 Ma, respectively; incremental heating of chemically homogeneous hornblende from the same sample yields a $^{40}Ar/^{39}Ar$ age of 12.42 Ma (Calzia, 1990).

The feldspar porphyry, quartz porphyry, and aplite facies are calc-alkaline and metaluminous to slightly peraluminuous. The feldspar porphyry and quartz porphyry facies yield similar REE patterns characterized by steep negative slopes and negative Eu anomalies. Volatile content increases from the feldspar porphyry to the quartz porphyry facies then decreases in the aplite facies; petrographic data suggests that volatiles were lost, probably by exsolution, during crystallization of the aplite facies. Colinear major and trace element variation diagrams, variation in Sr_i ratios, positive correlation between Sr_i and Rb/Sr ratios, and uniform but high Pb isotopic ratios suggest that the feldspar porphyry and quartz porphyry facies crystallized from a single granitic melt derived from an isotopically heterogeneous source region; high $^{207}Pb/^{204}Pb$ ratios suggest that this source region included Precambrian material. Sr and Pb isotopic data, combined

with trace element and petrographic data, suggest that the aplite melt was an open geochemical system during crystallization of the aplite facies. Stratigraphic reconstruction of the country rocks in the Kingston Range indicates that these granitic melts were emplaced at shallow (~4 km) crustal levels (Calzia, 1990).

Return to the vehicles, CAREFULLY turn around, and return to Horse Thief Springs. Drive 0.1 mi west of the ranch house(s) and turn north onto a dirt road along the west side of a corral. Last car, please close the gate.

Drive 6.2 mi north and park in Airport Wash. Charleston Peak and the Spring Mountains are visible on the skyline just north of the corral; the low hills east of the corral are miogeoclinal rocks in the upper plate of the Kingston Range detachment fault. Tall pyramid-shaped peak on the west side of the road 3.6 mi north of the corral is a satellite pluton of the granite of Kingston Peak.

Stop 3–3. Volcanic rocks in the Resting Springs Formation

Volcanic rocks in the Resting Springs Formation consist of porphyritic andesite flows, interbedded with rare basalt lenses and white lithic tuff, unconformably overlain by volcanic breccia of andesite, basalt, and latite cobbles in a matrix of calcareous tuff. Biotite from andesite flows east of this stop yields K-Ar ages of 12.1–12.5 Ma (Calzia, 1991).

These volcanic rocks are calc-alkalic and are divided into two magmatic suites based on geochemical data. Alkali-rich andesite and trachyte flows in the northern and eastern Kingston Range are metaluminuous and yield high and variable Sr_i ratios that average 0.7083. Andesite and trachyandesite (latite) flows in central Kingston Range are peraluminuous and yield an average Sr_i ratio of 0.7077. Alkalic basalt sills in these flows are metaluminuous and yield a Sr_i ratio of 0.7073. Chondrite-normalized REE patterns of all of these rocks are similar and form steep negative slopes with no Eu anomaly. Pb isotopic ratios are more radiogenic than present-day average crust and most volcanic rocks in the southern Death Valley region. Uniform $^{206}Pb/^{204}Pb$ and $^{208}Pb/^{204}Pb$ ratios imply that the volcanic rocks have a common source; high $^{207}Pb/^{204}Pb$ ratios suggest that Precambrian material was involved in their evolution. These data, combined with trace element ratios, suggest that andesite, trachyte, and trachyandesite flows in the Resting Springs Formation were derived from a lithospheric mantle source; the basalt sills were derived from the asthenosphere.

Return to the main road at the corral. REMEMBER; last car, please close the gate.

Turn west on the main road and return to the Crystal Spring mine and the Smith Talc Road. Turn south from the Smith Talc Road onto a dirt road ~5.0 mi west of the Crystal Spring mine. The east end of the Alexander Hills, with a white patch of talc, is at 12 o'clock.

Drive 3.0 mi south on the dirt road and take the west fork toward the talc mine in the Alexander Hills.

Turn east toward the Kingston Range and the mouth of Porcupine Wash ~1.2 mi south of the fork at the talc mine.

Continue into Porcupine Wash and park at the corral at the end of the road.

Stop 3–4. Mafic xenoliths and the petrogenesis of the granite of Kingston Peak

Mafic xenoliths occur as rounded to irregular-shaped clots (up to 10 mm across) or teardrop-shaped inclusions (up to several cm long) in the feldspar porphyry and quartz porphyry facies of the granite of Kingston Peak. The xenoliths are widely scattered throughout the batholith but are most common in Porcupine Wash.

The mafic xenoliths consist of fine-grained subhedral andesine, hypersthene altered to chlorite, and abundant opaque oxides. Green hornblende, up to 6 mm long, is common. Spherulitic biotite forms a reaction rim around an unidentified mafic mineral that is completely altered to chlorite or actinolite with clots of reddish brown opaque stain. The shape of the biotite reaction rim suggests that the original mineral was amphibole. A few embayed and in part skeletal crystals have inclined extinction and clinopyroxene habit; these crystals are completely altered to chlorite, biotite, and opaque oxides and could not be identified with certainty (Calzia, 1990).

The feldspar porphyry facies adjacent to mafic xenoliths in Porcupine Wash is generally finer grained and contains less plagioclase that is more sodic than normal for this rock. Green hornblende, locally with blue pleochroism, is common; the change in pleochroism indicates that the hornblende is more sodic than other hornblendes in this facies. Rare orthopyroxene crystals in the granite are completely surrounded by opaque oxides and are altered to talc or actinolite. The abundance and texture of the orthopyroxene crystals suggest that they are xenocrysts that were not in equilibrium with the adjacent melt during crystallization. These observations, combined with the abundance of orthopyroxene xenocrysts in the feldspar porphyry facies, indicate that some type of magmatic and chemical interaction occurred between the granitic melts and the mafic xenoliths in the Kingston Range (Calzia, 1990).

Identical REE patterns and Sr_i ratios but lower Pb isotopic ratios suggest that mafic xenoliths in the granite of Kingston Peak were derived from similar but less radiogenic source rocks as volcanic rocks in the Resting Springs Formation. The high concentration of Na_2O and Rb suggest that the xenolith melt was contaminated by crustal melt(s); nonlinear major and trace element variation diagrams, however, preclude mixing of the xenolith and granitic melts (Calzia, 1990).

Chemical and isotopic data limit the possible source rock(s) of the granite of Kingston Peak. Rb/Sr ratios in the feldspar porphyry and quartz porphyry facies are low (0.63–0.90) and variable; Sr_i varies from 0.7085–0.7126. Given that the average mineral/melt partition coefficients (Kd) of Rb and Sr in feldspars are 0.38 and 9.40, respectively, possible source rock(s) must also have a low Rb/Sr ratio to yield Rb/Sr ratios less than 1 during partial melting. Lower crustal and mantle xenoliths in

the Death Valley and Mojave Desert regions have Rb/Sr ratios less than 1 but are much less radiogenic, with respect to Sr, than the granite of Kingston Peak. These data preclude a lower crust and (or) mantle source for the granite of Kingston Peak.

Lead and strontium isotopic data suggest that the granite of Kingston Peak was derived from upper crustal rocks. Proterozoic crustal rocks and Mesozoic intrusive rocks in the northern Mojave Desert yield similar $^{206}Pb/^{204}Pb$, $^{207}Pb/^{204}Pb$, and $^{208}Pb/^{204}Pb$ ratios that form overlapping elliptical fields elongated along the 1700 Ma reference isochron. Wooden et al. (1988) concluded, based on this as well as other data, that the Mesozoic intrusive rocks were derived from the Proterozoic rocks. The granite of Kingston Peak also yields similar Pb isotopic ratios that form a steep linear pattern at an acute angle to the 1700 and the 100 Ma reference isochrons; this linear pattern also aligns with and includes the Pb isotopic ratios of coeval volcanic rocks from the Resting Springs Formation. These data suggest that the granite of Kingston Peak may be derived from the Proterozoic crustal rocks, or it may be derived from Mesozoic intrusive rocks that contain an inherited Proterozoic component; unfortunately, it is not possible to discriminate between Proterozoic or Mesozoic source rocks based on the Pb isotopic data. The pronounced linear pattern of the granite and the volcanic rocks suggests that these rocks plot along a mixing line that involves the Proterozoic and Mesozoic rocks as well as a less radiogenic component. Chemical and isotopic data suggest that the volcanic rocks in the Resting Springs Formation were generated in the asthenosphere and have interacted with lithospheric rocks during their ascent. If so, then these volcanic rocks may represent the less radiogenic component that interacted with more radiogenic Proterozoic and Mesozoic rocks in the upper crust to produce the granite of Kingston Peak.

Partial melting models are consistent with this conclusion. Simple batch melting calculations, using Rb, Ba, Sr, and REE data, indicate that the feldspar porphyry and quartz porphyry facies may be derived by a 10%–90% (average 35%–45%) partial melt of the Teutonia Batholith. Partial melts of Proterozoic crustal rocks yield results that are not geologically reasonable (i.e., the fraction of melt is greater than one or a negative number). Partial melts of a source rock as heterogeneous as the Teutonia Batholith may result in successive batches of granitic magma with variable chemical and isotopic compositions and is consistent with the chemical and isotopic variations and strong LREE enrichment of the feldspar porphyry and quartz porphyry facies. In addition, this model implies that the Teutonia Batholith is beneath the Kingston Range, consistent with regional isostatic gravity data.

Return to Smith Talc Road. The Valjean Hills are at 9 o'clock; the Avawatz Mountains form the skyline beyond the Valjean Hills. The Alexander Hills are at 12 o'clock and the Nopah Range is at 2 o'clock.

Turn west on the Smith Talc Road and drive 1.1 mi to the intersection of the Mesquite Valley Road.

Turn north on the Mesquite Valley Road and drive ~7 mi to the intersection of the Old Spanish Trail Highway. CAREFUL, it is a tight turn onto Mesquite Valley Road. The Nopah Range is at 9 o'clock; the Spring Mountains are at 1–2 o'clock.

Turn east on the Old Spanish Trail Highway and drive ~20 mi to the intersection of Highway 160 in Nevada.

Turn east on Highway 160 and return to Las Vegas.

ACKNOWLEDGMENTS

REFERENCES CITED

Abbott, E.W., 1971, Structural geology of the southern Silurian Hills, San Bernardino County, California [M.S. thesis]: Rice University, 48 p.

Allmendinger, R.W., and seven others, 1987, Overview of the COCORP 40°N transect, western United States: The fabric of an orogenic belt: Geological Society of America Bulletin, v. 98, p. 308–319.

Almashoor, S.S., 1980, The petrology of a quartz monzonite pluton in the southern Greenwater Range, Inyo County, California [Ph.D. dissertation]: Pennsylvania State University, 155 p.

Armstrong, R.L., 1970, Geochronology of Tertiary igneous rocks, eastern Basin and Range province, western Utah, eastern Nevada, and vicinity, USA: Geochimica et Cosmochimica Acta, v. 34, p. 203–232.

Asmerom, Yemane, and five others, 1990, Rapid uplift and crustal growth in extensional environments: An isotopic study from the Death Valley region, California: Geology, v. 18, p. 223–226.

Asmerom, Yemane, Jacobsen, S.B., and Wernicke, B.P., 1994, Variations in magma source region during large-scale continental extension, Death Valley region, western United States: Earth and Planetary Science Letters, v. 125, p. 235–254.

Barker, J.M., and Wilson, J.L., 1975, Borate deposits in the Death Valley region: Nevada Bureau of Mines and Geology Report 26, p. 23–32.

Beckerman, G.M., Robinson, J.P., and Anderson, J.L., 1982, The Teutonia Batholith: A large intrusive complex of Jurassic and Cretaceous age in the eastern Mojave Desert, California, *in* Frost, E.G. and Martin, D.L., eds., Mesozoic-Cenozoic tectonic evolution of the Colorado River region, California, Arizona, and Nevada: San Diego, Cordilleran Publishers, p. 205–220.

Bishop, K.M., Davis, G.A., Fowler, T.K., and Parke, Mary, 1991, Late Tertiary geology of the Halloran Hills area, southeast California: Problems in deciphering the geometric evolution of an extended terrane: Geological Society of America Abstracts with Program, v. 23, p. A82.

Brady, R.H., 1985, Cenozoic geology of the northern Avawatz Mountains between the Garlock and Death Valley fault zones, southern Death Valley, California: Implications as to Late Cenozoic tectonism [Ph.D. dissertation]: Davis, University of California, 252 p.

Brady, R.H., 1990, Stratigraphy and structure at the intersection of the Garlock and Death Valley fault zones, northern Avawatz Mountains, California: *in* Reynolds, R.E., Wells, S.G., and Brady, R.H., eds., At the end of the Mojave: Quaternary studies in the eastern Mojave Desert: San Bernardino County Museum Guidebook, p. 119–128.

Brudos, T.C., and Davis, G.A., 1992, Geology of a Tertiary extensional breakaway zone, eastern Mojave Desert, California: Geological Society of America Abstracts with Programs, v. 24, p. 10.

Burchfiel, B.C., and Davis, G.A., 1971, Clark Mountain thrust complex in the Cordillera of southeastern California, *in* Elders, W.A., ed., Geological

excursions in southern California: Riverside, University of California Campus Museum Contributions Number 1, p. 1–28.

Burchfiel, B.C., and Davis, G.A., 1988, Mesozoic thrust faults and Cenozoic low-angle normal faults, eastern Spring Mountains, Nevada, and Clark Mountains thrust complex, California, in Weide, D.L., and Faber, M.L., eds., This extended land: Geological journeys in the southern Basin and Range: Geological Society of America, Cordilleran Section, Field Trip Guidebook, p. 87–105.

Burchfiel, B.C., Walker, J.D., and Davis, G.A., 1983, Kingston Range and related detachment faults: A major "breakaway" zone in the southern Great Basin: Geological Society of America Abstracts with Programs, v. 15, p. 536.

Burchfiel, B.C., and seven others, 1985, The Kingston Range detachment system: Structures at the eastern edge of the Death Valley extensional zone, southeastern California: Geological Society of America Abstracts with Programs, v. 17, p. 345.

Butler, P.R., 1984, Geology, structural history, and fluvial geomorphology of the southern Death Valley fault zone, Inyo and San Bernardino Counties, California [Ph.D. dissertation]: Davis, University of California, 122 p.

Calzia, J.P., 1974, Igneous geology of a part of the southeastern Owlshead Mountains, San Bernardino County, California [M.S. thesis]: University of Southern California, 76 p.

Calzia, J.P., 1990, Geologic studies in the Kingston Range, southern Death Valley region, California [Ph.D. dissertation]: Davis, University of California, 230 p.

Calzia, J.P., 1991, Geology of the Kingston Range, southern Death Valley, California, in Reynolds, R.E., compiler, Crossing the borders: Quaternary studies in eastern California and southwestern Nevada: San Bernardino County Museum Mojave Desert Quaternary Research Center Field Trip Guidebook, p. 176–188.

Calzia, J.P., 1994, Petrogenesis of a middle Miocene rapakivi granite, Death Valley, California, USA: International Mineralogical Association 16th General Meeting, Pisa, Italy, Abstracts Volume, p. 62.

Calzia, J.P., and Finnerty, A.A., 1984, Geologic and geochemical reconnaissance of Late Tertiary granitic plutons, Death Valley, California: Geological Society of America Abstracts with Programs, v. 16, p. 461.

Calzia, J.P., and Rämö, O.T., 1997, The granite of Kingston Peak: Petrogenesis of a middle Miocene postsubduction granite in the southern Death Valley region, California: EUG9 Abstracts, Abstract Supplement no. 1, Terra Nova, v. 9, p. 458.

Calzia, J.P., Blakely, R.J., and Jachens, R.C., 1991, Miocene magmatism and extension in Ibex Pass, southern Death Valley, California: Eos, v. 72, p. 469.

Calzia, J.P., Verosub, K.L., and Jachens, R.C., 1986, Tilting and faulting of the late Miocene Kingston Peak granite, southern Death Valley, California: Eos, v. 67, p. 1189.

Calzia, J.P., and four others, 1987, Mineral resources of the Kingston Range Wilderness Study Area, San Bernardino County, California: U.S. Geological Survey Bulletin 1709, 21 p.

Castor, S.B., 1991, Rare earth deposits in the southern Great Basin, in Raines, G.L., Lisle, R.E., Schafer, R.W., and Wilkinson, W.H., eds., Geology and ore deposits of the Great Basin: Geological Society of Nevada, Symposium Proceedings, p. 523–528.

Cheadle, M.J., and eight others, 1986, The deep crustal structure of the Mojave Desert, California, from COCORP seismic reflection data: Tectonics, v. 5, p. 293–320.

Christiansen, R.L., and Lipman, P.W., 1972, Cenozoic volcanism and plate-tectonic evolution of the western United States: Philosophical Transactions, Royal Society of London, v. A271, p. 249–284.

Crow, H.C., 1984, Geochemistry of shonkinites, syenites, and granites associated with the Sulfide Queen carbonatite body, Mountain Pass, California [M.S. thesis]: Las Vegas, University of Nevada, 56 p.

Davis, G.A., and Fleck, R.J., 1977, Chronology of Miocene volcanic and structural events, central Owlshead Mountains, eastern San Bernardino

County, California: Geological Society of America Abstracts with Programs, v. 9, p. 409.

Davis, G.A., and seven others, 1993, Pluton pinning of an active detachment fault system, eastern Mojave Desert, California: Geology, v. 21, p. 627–630.

DeWitt, E., Armstrong, R.L., Sutter, J.F., and Zartman, R.E., 1984, U-Th-Pb, Rb-Sr, and Ar-Ar mineral and whole-rock isotopic systematics in a metamorphosed granitic terrane, southeastern California: Geological Society of America Bulletin, v. 95, p. 723–739.

DeWitt, E., Kwak, L.M., and Zartman, R.E., 1987, U-Th-Pb and $^{40}Ar/^{39}Ar$ dating of the Mountain Pass carbonatite and alkalic igneous rocks, southeast California: Geological Society of America Abstracts with Programs, v. 19, p. 642.

Dohrenwend, J.C., McFadden, L.D., Turrin, B.D., and Wells, S.G., 1984, K-Ar dating of the Cima volcanic field, eastern Mojave Desert, California: Late Cenozoic volcanic history and landscape evolution: Geology, v. 12, p. 163–167.

Eberly, L.D., and Stanley, T.B., Jr., 1978, Cenozoic stratigraphy and geologic history of southwestern Arizona: Geological Society of America Bulletin, v. 89, p. 921–940.

Elliott, G.S., 1986, Eary Proterozoic high grade metamorphic rocks of Willow Wash, New York Mountains, southeastern California [MS thesis]: San Jose, California State University, 110 p.

Fowler, T.K., and Calzia, J.P., 1999, Kingston Range detachment fault, southeastern Death Valley region, California: Relation to Tertiary deposits and reconstruction of initial dip, in Wright, L.A., and Troxel, B.W., eds., Cenozoic basins of the Death Valley region: Geological Society of America Special Paper 333, p. 245–257.

Fowler, T.K., Friedmann, S.J., Davis, G.A., and Bishop, K.M., 1995, Two-phase evolution of the Shadow Valley basin, southeastern California: A possible record of footwall uplift during extensional detachment faulting: Basin Research, v. 7, p. 165–179.

Friedmann, S.J. 1996, Miocene strata below the Shadow Valley basin fill, eastern Mojave Desert, California, in Reynolds, R.E., and Reynolds, J., Punctuated chaos in the northeastern Mojave Desert: San Bernardino County Museum Association Quarterly, v. 43, p. 123–126.

Friedmann, S.J., and Burbank, D.W., 1992, Active footwall uplift recorded in a supradetachment basin: The Miocene Shadow Valley basin: Eos, v. 73 (Supplement), p. 549.

Friedmann, S.J., and six others, 1994, Stratigraphy and gravity glide elements of a Miocene supradetachment basin, Shadow Valley, east Mojave Desert: Geological Society of America Cordilleran Section Guidebook, p. 302–318.

Friedmann, S.J., Davis, G.A., and Fowler, T.K., 1996, Geometry, paleodrainage, and geologic rates from the Miocene Shadow Valley supradetachment basin, eastern Mojave Desert, California, in Beratan, K.K., ed., Reconstructing the history of Basin and Range extension using sedimentology and stratigraphy: Geological Society of America Special Paper 303, p. 85–105.

Glazner, A.F., and Ussler, W., III, 1988, Trapping of magma at midcrustal density discontinuities: Geophysical Research Letters, v. 15, p. 673–675.

Haefner, Richard, 1972, Igneous history of a rhyolite lava-flow series near Death Valley, California [Ph.D. dissertation]: Pennsylvania State University, 281 p.

Hammond, J.G., 1986, Geochemistry and petrogenesis of Proterozoic diabase in the southern Death Valley region of California: Contributions to Mineralogy and Petrology, v. 93, p. 312–321.

Haxel, G.B., in press, Ultrapotassic rocks, carbonatite, and rare earth element deposit, Mountain Pass, California, in Theodore, T.G., ed., Geology and mineral resources of the East Mojave National Scenic Area, San Bernardino County, California: U.S. Geological Survey Bulletin 2160.

Heaman, L.M., and Grotzinger, J.P., 1992, 1.08 Ga diabase sills in the Pahrump Group, California: Implications for the development of the Cordilleran miogeocline: Geology, v. 20, p. 637–640.

Hessler, M.J., and Friend, L.D., 1986, Geology of the Valjean Hills, southeastern Death Valley region, San Bernardino County, California [senior thesis]: Sonoma, California State University, 56 p.

Hewett, D.F., 1940, New formation names to be used in the Kingston Range, Ivanpah Quadrangle, California: Washington Academy of Science Journal, v. 30, p. 239–240.

Hewett, D.F., 1956, Geology and mineral resources of the Ivanpah Quadrangle, California and Nevada: U.S. Geological Survey Professional Paper 275, 172 p.

Hildreth, Wes, 1981, Gradients in silicic magma chambers: Implications for lithospheric magmatism: Journal of Geophysical Research, v. 86, p. 10153–10192.

Hillhouse, J.W., 1987, Late Tertiary and Quaternary geology of the Tecopa basin, southeastern California: U.S. Geological Survey Miscellaneous Investigations Map I-1728, scale 1:48,000.

Holm, D.K., Pavlis, T.L., and Topping, D.J., 1994, Black Mountains crustal section, Death Valley region, California, *in* McGill, S.F., and Ross, T.M., eds., Geological investigations of an active margin: Geological Society of America Cordilleran Section Guidebook, San Bernardino, California, March 21–23, 1994, p. 31–54.

Holm, D.K., Snow, J.K., and Lux, D.R., 1992, Thermal and barometric constraints on the intrusive and unroofing history of the Black Mountains: Implications for timing, initial dip, and kinematics of detachment faulting in the Death Valley region, California: Tectonics, v. 11, p. 507–522.

Huppert, H.E., and Sparks, R.S., 1988, The generation of granitic magmas by intrusion of basalt into continental crust: Journal of Petrology, v. 29, p. 599–624.

Irvine, T.N., and Baragar, W.R.A., 1971, A guide to the chemical classification of common volcanic rocks: Canadian Journal of Earth Sciences, v. 8, p. 523–548.

Jachens, R.C., and Calzia, J.P., 1998, A geophysical analysis of the Garlock Fault, *in* Calzia, J.P., and Reynolds, R.E., eds., Finding faults in the Mojave: San Bernardino County Museum Association Quarterly, v. 45, p. 36–41.

Johnson, B.K., 1957, Geology of a part of the Manly Peak Quadrangle, southern Panamint Range, California: University of California Publications in the Geological Sciences, v. 30, p. 353–424.

Kupfer, D.H., 1960, Thrust faulting and chaos structure, Silurian Hills, San Bernardino County, California: Geological Society of America Bulletin, v. 71, p. 181–214.

Labotka, T.C., 1981, Petrology of an andalusite-type regional metamorphic terrane, Panamint Mountains, California: Journal of Petrology, v. 22, p. 261–296.

Labotka, T.C., and Albee, A.L., 1988, Metamorphism and tectonics of the Death Valley region, California and Nevada, *in* Ernst, W.G., ed., Metamorphism and crustal evolution of the western United States: Englewood, New Jersey, Prentice-Hall, p. 715–736.

Lachenbruch, A.H., and Sass, J.H., 1977, Heat flow in the United States and the thermal regime of the crust, *in* Heacock, J.G., ed., The Earth's crust: American Geophysical Union Monograph 20, p. 626–675.

Lachenbruch, A.H., Sass, J.H., and Galanis, S.P., Jr., 1985, Heat flow in southernmost California and the origin of the Salton Trough: Journal of Geophysical Research, v. 90, p. 6709–6736.

Laibidi, E.H., 1981, Structural geology of the Resting Spring Range, Inyo County, Death Valley region, eastern California [M.S. thesis]: Pennsylvania State University, 139 p.

Lanphere, M.A., Wasserburg, G.J.F., Albee, A.L., and Tilton, G.R., 1964, Redistribution of strontium and rubidium isotopes during metamorphism, World Beater Complex, Panamint Range, California, *in* Craig, H., Miller, S.L., and Wasserburg, G.J.F., eds., Isotopic and cosmic chemistry: Amsterdam, North Holland Publishing Company, p. 269–320.

Louie, J., and eight others, 1992, 7 Ma age of Tecopa lake and tectonic quiescence from seismic stratigraphy east of Death Valley, California: Eos, v. 73, p. 548.

Lucchitta, I., 1985, Heat and detachment in core-complex extension, *in* Conference on heat and detachment in crustal extension on continents and planets: Lunar and Planetary Institute Contribution 575, p. 64–68.

Lucchitta, I., 1990, Role of heat and detachment in continental extension as viewed from the eastern Basin and Range Province in Arizona: Tectonophysics, v. 174, p. 77–114.

Luth, W.C., Jahns, R.H., and Tuttle, O.F., 1964, The granite system at pressures of 4 to 10 kilobars: Journal of Geophysical Research, v. 69, p.759–773.

Mason, J.P., 1948, Geology of the Tecopa area, southeastern California: Geological Society of America Bulletin, v. 59, p. 333–352.

McCarthy, J., and Thompson, G.A., 1988, Seismic imaging of extended crust with emphasis on the western United States: Geological Society of America Bulletin, v. 100, p. 1361–1374.

McMackin, M.R., 1997, Late Tertiary evolution of the southern Death Valley fault system: The origin of the Tecopa hump, a tectonic dam on the Amargosa River, *in* Reynolds, R.E., and Reynolds, J., eds., Death Valley: The Amargosa route: San Bernardino County Museum Association Quarterly, v. 44, p. 37–42.

Miyashiro, A., 1974, Volcanic rock series in island arcs and active continental margins: American Journal of Science, v. 274, p. 321–355.

Morrison, R.B., 1991, Quaternary stratigraphic, hydrologic, and climatic history of the Great Basin, with emphasis on Lakes Lahontan, Bonneville, and Tecopa, *in* Morrison, R.D., ed., Quaternary nonglacial geology: Conterminous U.S: Geological Society of America, The Geology of North America, v. K-2, p. 283–320.

Niemi, N.A., and four others, 1999, Magnitude and timing of extreme continental extension, central Death Valley region, California: U.S. Geological Survey Open-File Report 99–153, p. 33–35.

Noble, L.F., 1941, Structural features of the Virgin Spring area, Death Valley, California: Geological Society of America, v. 52, p. 941–1000.

Novak, G.G., 1967, Petrography and mineralogy of a rapakivi quartz monzonite pluton, Eagle Mountain Quadrangle, California [M.S. thesis]: Pennsylvania State University, 69 p.

Olson, J.E., Shawe, D.R., Pray, L.C., and Sharp, W.N., 1954, Rare-earth mineral deposits of the Mountain Pass district, San Bernardino County, California: U.S. Geological Survey Professional Paper 261, 75 p.

Otton, J.K., 1977, Geology of the central Black Mountains, Death Valley, California: The turtleback terrane [Ph.D. dissertation]: Pennsylvania State University, 155 p.

Prave, A.R., and McMackin, M.R., 1999, Depositional framework of mid to late Miocene strata, Dumont Hills and southern margin Kingston Range: Implications for the tectonostratigraphic evolution of the southern Death Valley region, *in* Wright, L.A., and Troxel, B.W., Cenozoic basins of the southern Death Valley region: Boulder, Colorado, Geological Society of America Special Paper 333, p. 259–275.

Rämö, O.T., and Calzia, J.P., 1998, Nd isotopic composition of cratonic rocks in the southern Death Valley region: Evidence for a substantial Archean source component in Mojavia: Geology, v. 26, p. 891–894.

Rämö, O.T., Calzia, J.P., and Kosunen, P.J., 2000, Geochemistry of Middle Jurassic–Late Cretaceous plutons in the southern Death Valley region, California: New insights into the origin of Cordilleran interior magmatism: Submitted to Contributions to Mineralogy and Petrology.

Rämö, O.T., Calzia, J.P., Wooden, J.L., and Kosunen, P.J., 1999, Origin of Phanerozoic granitoid magmatism in southern Death Valley, California, USA, *in* Barbarin, B., ed., The origin of granites and related rocks: Fourth Hutton Symposium Abstracts Clermont-Ferrand, France, Documents du BRGM 209, p. 181.

Scott, R.K., 1985, Stratigraphy and depositional environments of a Neogene playa-lake system, China Ranch beds, near Death Valley, California [M.S. thesis]: University Park, Pennsylvania State University, 240 p.

Scott, R.K., Wright, L.A., and Drake, R.E., 1988, Thrust fault-related monolithologic breccias and cyclic playa-lake deposits in the Miocene China Lake basin, Death Valley region, California: Geological Society of America Abstracts with Programs, v. 20, p. 229.

Serpa, L., deVoogd, B., Wright, L.W., and Troxel, B.W., 1986, A model for the structural evolution of the central Death Valley basin from COCORP seismic data: Geological Society of America Abstracts with Programs, v. 18, p. 182.

Serpa, L., and six others, 1988, Structure of the central Death Valley pull-apart basin and vicinity from COCORP profiles in the southern Great Basin: Geological Society of America Bulletin, v. 100, p. 1437–1450.

Sonder, L.J., England, P.C., Wernicke, B.P., and Christiansen, R.L., 1987, A physical model for Cenozoic extension of western North America, in Coward, M.P., Dewey, J.F., and Hancock, P.L., eds., Continental extensional tectonics: Geological Society of London Special Publication 28, p. 187–201.

Stewart, J.H., 1980, Geology of Nevada: Nevada Bureau of Mines and Geology Special Publication Number 4, 136 p.

Topping, D.J., 1993, Paleographic reconstruction of the Death Valley extended region: Evidence from Miocene large rock-avalanche deposits in the Amargosa chaos basin, California: Geological Society of America Bulletin, v. 105, p. 1190–1213.

Troxel, B.W., and Butler, P.R., 1998, Tertiary and Quaternary fault history of the intersection of the Garlock and Death Valley fault zones, southern Death Valley, California, in Calzia, J.P., and Reynolds, R.E., eds., Finding faults in the Mojave: San Bernardino County Museum Association Quarterly, v. 45, p. 91–98.

Troxel, B.W., and Calzia, J.P., 1994, Geology of the middle Miocene Ibex Pass volcanic field, southern Death Valley, California: Geological Society of America Abstracts with Programs, v. 26, p. 99.

Turrin, B.D., Dohrenwend, J.C., Drake, R.E., and Curtis, G.H., 1985, K-Ar ages from the Cima volcanic field, eastern Mojave Desert, California: Isochron/West, v. 44, p. 9–16.

U.S. Geological Survey, 1991, Evaluation of metallic mineral resources and their geographic controls in the Eastern Mojave Scenic Area, San Bernardino County, California: U.S. Geological Survey Open-File Report 91–427, 278 p.

Wagner, D.L., 1988, Evidence for late Cenozoic extension across Wingate Wash, Death Valley region, southeastern California, in Gregory, J.L., and Balwin, E.J., eds., Geology of the Death Valley region: South Coast Geological Society Field Trip Guidebook, p. 243–259.

Wagner, D.L., 1994, Extension and syntectonic volcanism in Wingate Wash, southeastern Death Valley region, California: Geological Society of America Abstracts with Programs, v. 26, p. 101.

Watson, K.D., Morton, D.M., and Baird, A.K., 1974, Shonkinite-syenite plutons, Mountain Pass, San Bernardino County, California: Geological Society of America Abstracts with Programs, v. 6, no. 3, p. 273.

Wernicke, B.P., 1981, Low-angle normal faults in the Basin and Range province: Nappe tectonics in an extended orogen: Nature, v. 291, p. 645–648.

Wernicke, B.P., 1985, Uniform-sense normal simple shear of the continental lithosphere: Canadian Journal Earth Science, v. 22, p. 108–125.

Wernicke, B.P., Axen, G.J., and Snow, J.K., 1988, Basin and Range extensional tectonics at the latitude of Las Vegas, Nevada: Geological Society of America Bulletin, v. 100, p. 1738–1757.

Wilhelms, D.E., 1963, Geology of part of the Nopah and Resting Spring Ranges, Inyo County, California [Ph.D. dissertation]: Los Angeles, University of California, 224 p.

Wilshire, H.G., 1990, Lithology and evolution of the crust-mantle boundary region in the southwestern Basin and Range province: Journal of Geophysical Research, v. 95, p. 649–665.

Wilshire, H.G., and six others, 1988, Mafic and ultramafic xenoliths from volcanic rocks of the western United States: U.S. Geological Survey Professional Paper 1443, 179 p.

Wooden, J.L., and Miller, D.M., 1990, Chronologic and isotopic framework for Early Proterozoic crustal evolution in the eastern Mojave Desert region, southeast California: Journal of Geophysical Research, v. 95, p. 20,113–20,146.

Wooden, J.L., and four others, 1988, Pb isotopic evidence for the formation of Proterozoic crust in the southwestern United States, in Ernst, W.G., ed., Metamorphism and crustal evolution of the western United States: New Jersey, Prentice-Hall, p. 69–86.

Wright, L.A., 1954, Geology of the Alexander Hills area, Inyo and San Bernardino Counties: California Division of Mines and Geology Bulletin 170, Map Sheet 17.

Wright, L.A., 1955, Rainbow Mountain breccias, Amargosa Valley, California: Geological Society of America Bulletin, v. 66, p. 1670.

Wright, L.A., 1968, Talc deposits of the southern Death Valley–Kingston Range region, California: California Division of Mines and Geology Special Report 95, 79 p.

Wright, L.A., 1976, Late Cenozoic fault patterns and stress fields in the Great Basin and westward displacement of the Sierra Nevada block: Geology, v. 4, p. 489–494.

Wright, L.A., 1977, Late Cenozoic fault patterns and stress fields in the Great Basin and westward displacement of the Sierra Nevada block: Comment and reply: Geology, v. 5, p. 388–392.

Wright, L.A., and Troxel, B.W., 1971, Thin-skinned megaslump model of Basin Range structure as applicable to the southwestern Great Basin: Geological Society of America Abstracts with Programs, v. 2, p. 758.

Wright, L.A., and Troxel, B.W., 1973, Shallow fault interpretation of Basin and Range structure, southwestern Great Basin, in DeJong, K.A., and Scholten, R., Gravity and tectonics: New York, Wiley-Interscience Publications, p. 397–407.

Wright, L.A., and Troxel, B.W., 1984, Geology of the north half of the Confidence Hills 15' Quadrangle, Inyo County, California: California Division of Mines and Geology Map Sheet 34, scale 1:24,000.

Wright, L.A., Burchfiel, B.C., Chapman, R.H., and Labotka, T.C., 1981, Geologic cross section from the Sierra Nevada to the Las Vegas valley, eastern California to southern Nevada: Geological Society of America Map and Chart Series MC-28M, 15 p.

Wright, L.A., Drake, R.E., and Troxel, B.W., 1984a, Evidence for the westward migration of severe crustal extension, southwestern Great Basin, California: Geological Society of America Abstracts with Programs, v. 16, p. 701.

Wright, L.A., Kramer, J.H., Thornton, C.P., and Troxel, B.W., 1984b, Type sections of new newly named volcanic units of the central Death Valley volcanic field, eastern California: California Division of Mines and Geology Map Sheet 34, p. 21–24.

Wright, L.A., and eight others, 1991, Cenozoic magmatic and tectonic evolution of the east-central Death Valley region, California, in Walawender, M.J., and Hanan, B.B., eds., Geologic excursions in southern California and Mexico: Geological Society of America Annual Meeting Guidebook, p. 93–126.

Wrucke, C.T., Jr., 1966, Precambrian and Cambrian rocks in the vicinity of Warm Springs Canyon, Panamint Range, California [Ph.D. dissertation]: Stanford University, 190 p.

Wyllie, P.J., 1971, Experimental limits for melting in the Earth's crust and upper mantle, in Heacock, J.G., ed., The structure and physical properties of the Earth's crust: American Geophysical Union Monograph 14, p. 279–301.

Zoback, M.L., Anderson, R.E., and Thompson, G.A., 1981, Cainozoic evolution of the state of stress and style of tectonics of the Basin and Range province of the western United States: Philosophical Transactions, Royal Society of London, v. A300, p. 407–434.